

Chapter 5

Natural and Anthropogenic Variations in the Radiation Balance

Abstract

The globally and annually averaged temperature response to anthropogenic as well as natural radiative forcing mechanisms since pre-industrial times is evaluated using a 1D coupled radiative-convective atmosphere ocean model. Although climate effects due to changing concentrations of greenhouse gases and aerosols are physically well-understood, accumulation of uncertainties causes a considerable range in potential surface temperature changes of 0.1 to 1.5 K in 1990 as compared to the pre-industrial era. For the solar influence we lack any physical mechanism. Therefore, we optimize the effects of several radiative forcing mechanisms simultaneously in terms of explained variance of the observed surface temperature. We find that 88% of the slightly smoothed temperature variations are explained for a combination of anthropogenic influence, 11-year sunspot cycle and long-term solar variations. It turns out that the solar signal is competitive with the magnitude of internal variability, rather than with the enhanced greenhouse effect since 1970. Statistically, we may limit the anthropogenic influence in 1990 at 0.4 ± 0.2 K. Here, the upper boundary is derived in case there is no solar influence, while the lower limit is calculated for twice the optimum solar impact.

5.1 Introduction

In the last two decades much attention has been given to possible human influence on climate. In the first place, there is a challenge for the scientific community to perceive the secrets of nature with respect to climate variations on timescales ranging from decades to millions of years. On the other hand, since climate change in the near future is relevant for society, the issue has been placed on the political agenda. The central question here is the rapidness of climate change in the forthcoming decades due to industrial activities. This, in fact, determines the necessity for taking measures by governments, preferably world-wide, such as the reduction of greenhouse gas emissions.

Unequivocal proof of human influence on climate has not yet been established, because year-to-year variations of global mean temperatures are roughly of the same order, namely about 0.5 °C, as the computed net enhanced greenhouse effect, using comprehensive climate models [e.g.

³R. van Dorland, and A.P. van Ulden, in *proceedings Sun and Climate: the influence of variations in solar activity on the earth's climate*, 1998.

Kiehl and Briegleb, 1993; Mitchell *et al.*, 1995]. Therefore, there is debate on the relative roles of the anthropogenic and natural signal. This is, in fact, called the attribution problem [IPCC, 1995].

Climate shows variations on all timescales for numerous reasons. Before the industrial revolution, only natural mechanisms could have affected climate. On timescales of million years, continental drift and substantial solar irradiance changes together with feedbacks on the carbon dioxide and methane concentrations are likely to have caused major climate variations. The occurrence of ice-ages and interglacial periods are thought to be related to orbital variations of the Earth in combination with interactions between the cryosphere and the earth's crust on a timescale of 100,000 years. On a timescale of a hundred years, which is considered in this paper, we may point to three mechanisms of natural variability. First, strong volcanic eruptions cause an increase of sulfate aerosols in the stratosphere during several years, thereby cooling the Earth's surface. Second, interactions between atmosphere, oceans and landsurface, including year-to-year variations of (sea-)ice, affect global annual mean temperature. The quasi-periodic El-Nino event is a clear example of such an interaction. Third, solar activity may play a role in climate variations.

We distinguish two marked solar cycles. Most pronounced is the 11 (or 22) years solar cycle of sunspot activity, which may affect climate via changes in solar irradiance [Lean, 1991] or via UV radiation variations, changing the amount of stratospheric ozone [Haigh, 1994]. Recently, Svensmark and Friis-Christensen [1997] have found a high correlation between cosmic ray intensities and cloud cover over oceans in extratropical regions during the period 1980-1995. However, they failed to specify the altitude of the suggested cloud cover variation of 3%, which is crucial for the determination of the climate effects, e.g. surface temperature changes. Cosmic ray intensity varies inversely with sunspot numbers. Dickinson [1975] proposed a possible link between the ionization effects of cosmic rays and sulfate aerosol formation and cloud nucleation in the vicinity of the tropopause. However, cirrus (high) cloud variations hardly affect global temperatures with the additional disadvantage of having the wrong sign. Also, long-term (about 80 years) variations of the length of the solar cycle between 8 and 12 years, the so-called Gleissberg cycle, may affect climate. Although effects of the latter have been found on global temperature in terms of good correlations and high explained variance, the physical mechanism(s) are by far not clear [Gilliland, 1982; Friis-Christensen and Lassen, 1991; Kelley and Wigley, 1992; Soon *et al.*, 1996]. Therefore, the role of solar activity on climate is still subjected to debate.

The concentrations of greenhouse gases and aerosol burden in the atmosphere have increased considerably since pre-industrial times. It has been recognized through isotope analysis that the observed increases of carbon dioxide (CO₂), methane (CH₄) and nitrous oxide (N₂O) are mainly caused by human activities. Chlorofluorocarbons (CFCs) are entirely anthropogenic, as these constituents were not present in the pre-industrial atmosphere. In addition to these long-lived and hence uniformly mixed greenhouse gases, anthropogenic emissions of NO_x, CO

in combination with CH₄ lead via a number of complex chemical reactions to the production of tropospheric ozone. Increases of ozone in the lower part of the atmosphere acts to warm the Earth's surface [IPCC, 1995; Lelieveld and Van Dorland, 1995; Roelofs *et al.*, 1997; Van Dorland *et al.*, 1997, Chapter 4]. On the other hand, the abundance of CFCs in the stratosphere causes ozone depletion, resulting in direct and significant stratospheric cooling and a small negative greenhouse effect [Van Dorland and Fortuin, 1994].

Sulfur emissions lead to the formation of sulfate aerosols. These particles are capable of reflecting shortwave radiation originating from the sun. In addition to this direct effect, (sulfate) aerosols may alter the size distribution of cloud droplets. The suggested decrease of average droplet radii results in both more reflection of solar radiation and a possible enhancement of the lifetime of clouds. These indirect mechanisms reinforce the cooling effect of sulfate aerosols. We emphasize here that the total aerosol effect is not well-known. Uncertainties are largely associated with estimates of the emissions of precursors [Benkovitz *et al.*, 1996] and with the parameterizations of chemical processes as well as the modelled transports. In addition, uncertainties in microphysical properties, such as size distributions and the interactions of aerosols with water vapour and droplets, hamper accurate estimates of the radiative effects. [Boucher *et al.*, 1995; Nemesure *et al.*, 1995; Van Dorland *et al.*, 1997, Chapter 4].

In this paper, we make an assessment of the possible mechanisms, which force climate change, including solar activity, over the period 1856-1996, for which global mean surface temperatures are available [Jones, 1994] (updated with 1995 and 1996, Figure 5.1). By using a one-column climate model, representing the global average atmosphere as well as ocean, we include our physical knowledge of the climate system as much as possible. This is done by performing time integrations using the considered forcing mechanisms in the period 1850-1997. Since we lack a physical explanation for the climate effects due to solar activity, we adopt several mechanisms to compute its climate response: solar constant variations, cloud cover changes, and variations of the average droplet radii. Then, we resort to a statistical technique to get amplitude as well as phase (for the Gleissberg cycle) information by optimizing the computed temperature responses to the observed temperature in terms of explained variance. The applicability of this technique is restricted to a linear forcing-response relationship and orthogonality of the investigated signals in order to discriminate between the causes. In section 5.2, we motivate the use of a 1-dimensional climate model by determining the important aspects of climate change. In section 5.3 we describe the climate model, its characteristics and the model input. Section 5.4 is devoted to our model results, evaluated with the help of statistical optimization of the explained variance. In section 5.5 we discuss the meaning of the results.

5.2 Radiation and Climate

The climate system can only communicate with outer space through the exchange of radiative energy. As a consequence, climate change is strongly linked with perturbations of atmospheric

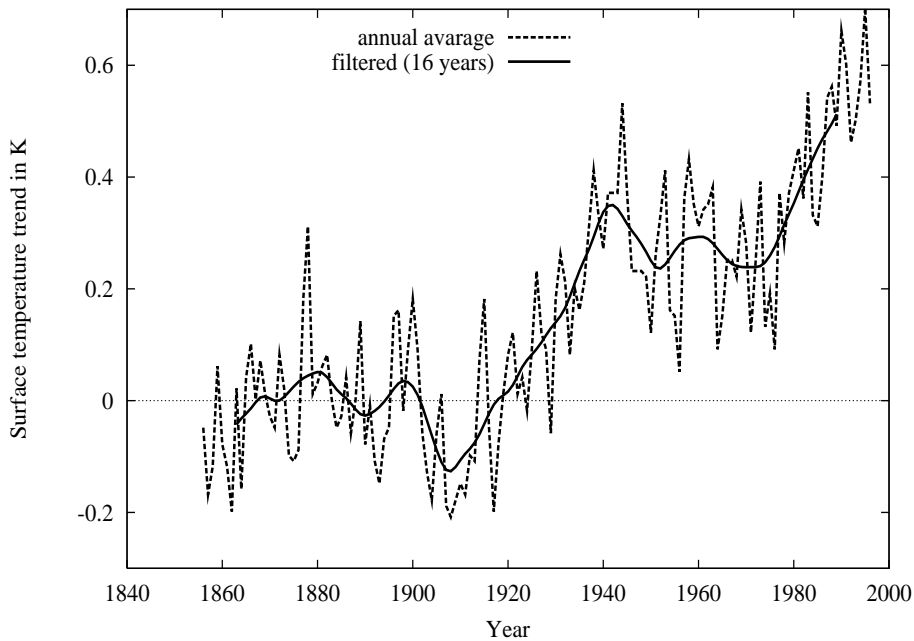


Figure 5.1: Observed global mean surface temperature relative to 1856-1900 [Jones, 1994]: annual mean (dashed line) and filtered with 16-year bicubic spline (solid line)

radiative transfer. Satellite measurements show that about 30% of the incoming solar (short-wave) radiation is reflected. The remaining part is absorbed by the atmosphere (23%) and by the Earth's surface (47%). This is converted into heat. In the equilibrium situation, this gain of energy is balanced by the same amount of outgoing infrared (longwave) radiation, which originates from the Earth's surface as well as the atmosphere.

Changes in atmospheric composition perturb the radiative transfer in the Earth's atmosphere, either in the longwave or in the shortwave spectral region. As a consequence, an imbalance at the top of atmosphere occur, that is a difference between net incoming shortwave radiation and outgoing infrared radiation. In order to restore the balance the temperature of the Earth's surface and atmosphere change until equilibrium is reached. While seeking a new equilibrium, temperature dependent processes in the climate system change as well, thereby amplifying or attenuating the temperature response with respect to the initial radiative perturbation. These so-called feedback mechanisms are dominantly present in the hydrological cycle due to the combination of large amounts of water at our planet and its strong impact on the radiation balance for all its phases (ice, liquid water and water vapour). The strongest positive feedback known is the increase of the amount of atmospheric water vapour in case of a temperature rise. Water vapour is an important greenhouse gas. Hence, it amplifies the warming by increases of

greenhouse gas concentration, and similarly, the cooling by an increase of sulfate burden. Also, the melting of land and especially sea ice cause a decrease in planetary albedo, resulting in more shortwave absorption by the climate system. Furthermore, clouds may change in several aspects such as cloud top height, the size distribution of droplet radii and therefore the lifetime and optical properties. The sign of the total cloud feedback is not well-known.

The best link between surface temperature change and radiative effect on a global scale, as can be derived from thermodynamic arguments, is given by the net radiative flux change at the tropopause level (approximately at 13 km altitude), the so-called radiative forcing. Above this level in the stratosphere, radiative equilibrium is reached within a few months, resulting in temperature adjustment, whereas this adjustment in the troposphere takes up to decades due to the large heat capacity of the oceans. In addition, the surface and troposphere are tightly coupled due to efficient vertical mixing processes with very short timescales and may therefore be considered as one thermodynamic (sub)system. This implies that global mean changes of radiation at the tropopause roughly determine the final temperature response at the Earth's surface.

The coupling between radiative forcing and equilibrium temperature response is called the climate sensitivity. For the present generation of 3D climate models, this climate sensitivity parameter is ranging from 0.3 to 1.1 K/Wm⁻². As this range is the result of differences in feedback mechanisms, the climate sensitivity for a specific model is independent of the mechanism behind the radiative forcing. This is even true for perturbations which are spatially confined to the northern hemisphere, such as the short-lived species ozone and sulfate aerosols [Ramasmamy and Chen, 1997; Roeckner, personal communication, 1997]. This implies that we may determine the relative climate effects of various mechanisms by evaluating their radiative forcings. Moreover, we may compute the subsequent temperature responses with relatively simple 1D climate models, in which the dynamical component is included in the climate sensitivity, e.g. changes in cloudiness with variations in the circulation. We assume these feedbacks either small or linear.

5.3 Model Description

5.3.1 Radiative-Convective Model

We use the KNMI 1D radiative-convective model (hereafter KRCM) to study the time evolution of the global average temperature due to changes in atmospheric composition and due to possible solar influences. The KRCM includes a radiation code, a convection algorithm, which organizes the non-radiative energy exchange between the Earth's surface and the troposphere, and an ocean model. The numerical experiments are performed with a vertical resolution of 27 atmospheric layers and 10 ocean layers. The water vapour feedback, enhancing the surface temperature response with a factor 1.8, is included.

We account for convective adjustment of the atmosphere as to simulate the observed tropospheric temperature gradient. These non-radiative fluxes, i.e. sensible and latent heat, are

computed from the surface energy balance. The scheme allows for the heat storage in the ocean layers. The energy exchange between the ocean layers is computed using the diffusion and (vertical) advection equation. The latter represents the global average upwelling of heat due to the thermohaline circulation and is kept constant in time. Hence, this term forces the background thermal structure of the ocean. For the diffusion coefficient we use $300 \text{ Wm}^{-1}\text{K}^{-1}$, which is comparable with empirical measurements of tracer transports in the ocean [Hoffert *et al.*, 1980]. The thickness of the ocean layers increases with depth in a logarithmic way to account for the typical thermal structure of the ocean in relation to the diffusion process. The total depth of the ocean model is 4000 m. The toplayer of 1.3 m represents the fast response of land surface, while the slowest response is due the deepest ocean layer of 2300 m.

The radiation code included in the KRCM is derived from the Morcrette radiative transfer model [Morcrette, 1991] and modified for climate modelling purposes (Chapter 3). The scheme, which is also part of the ECHAM4 climate model (MPI, Hamburg) [Roeckner *et al.*, 1996], includes the radiative effects of clouds, water vapour, ozone and the well-mixed greenhouse gases CO_2 , CH_4 , N_2O as well as 16 CFC's, HCFC's, HFC's. Also, the optical and longwave parameters for 11 aerosol components based on the Global Aerosol Data Set [d'Almeida *et al.*, 1991] have been incorporated. The longwave radiative transfer computations utilize a broad-band flux emissivity method with 6 spectral intervals, covering the spectrum between 0 and 2820 cm^{-1} . In the shortwave part of the model a two-stream formulation has been employed together with the photon path distribution method [Fouquart and Bonnel, 1980] in 2 spectral intervals, the visible (0.25-0.68 μm) and the near-infrared (0.68-4.0 μm) region.

5.3.2 Model Characteristics

Our climate model should represent at least two aspects of the real world: that is average climate and the climate response in amplitude as well as time-lag to radiative perturbations. We tuned our model as much as possible towards the presently observed global mean climatology. Typical profiles of water vapour and temperature are adopted from Oort [1983]. Clouds are defined in three model layers, the so-called low, middle and high clouds, for which the liquid water content and fractional coverage are specified. The ensemble of the mentioned entities are brought into agreement with the radiative fluxes, as measured by a number of satellites, the Earth Radiation Budget Experiment (ERBE), as well as ground based data for the surface energy flows. Furthermore, we have determined the frequency characteristics of the model's climate system to estimate the parameters of the ocean model, such as the thickness of the highest ocean layers as well as the diffusion coefficient, regulating the energy exchange.

In order to describe the frequency characteristics of the coupled atmosphere-ocean/land-surface system, we performed experiments in which we feed the model with monochromatic signals ranging from 1 to 1000 years. The forcing mechanisms were either a variation of the solar constant, a shortwave perturbation, or a variation of the CO_2 concentration, a merely longwave

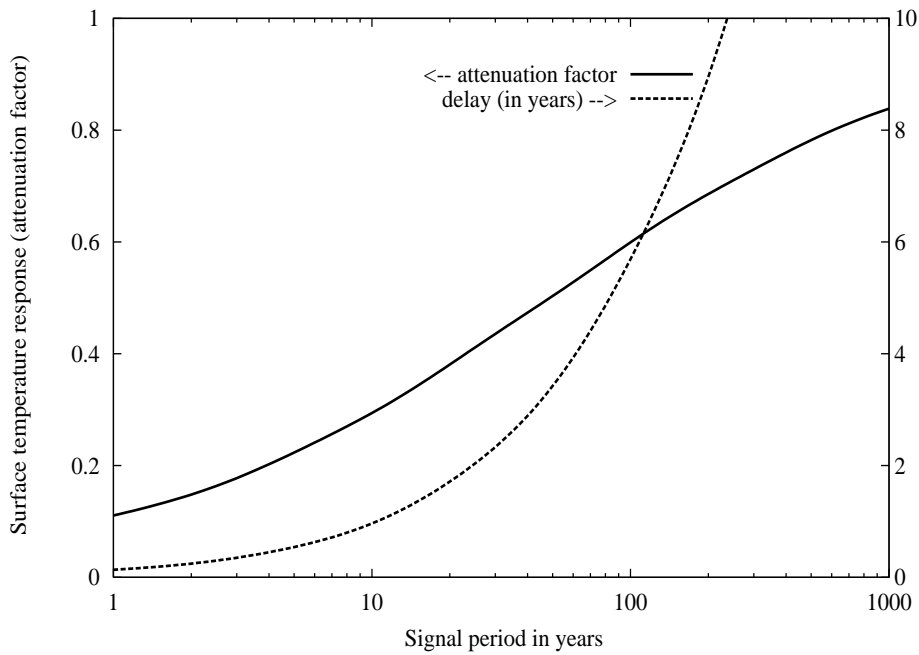


Figure 5.2: Surface temperature response as attenuation factor of equilibrium response (solid line) and time-lag in years (dashed line) as function of the signal period in years

perturbation. No essential differences between the surface temperature responses of both signals were found, although these forcing mechanisms affect the energy flows in the surface balance differently. This confirms the fact that the forcing-response relationship is unique. In Figure 5.2 we have plotted the amplitude as well as time-lag of the temperature response of the upper ocean layer. The amplitude of the response has been normalized with the equilibrium temperature response due to a "step forcing" for the maximum amplitude of the periodic signal. The equilibrium response is similar to the multiplication of the radiative forcing and the climate sensitivity parameter, which is 0.54 K/Wm^{-2} in our model. The amplitude increases with the period of the signal. The full equilibrium response is reached for a signal with an infinite period, while the amplitude of the seasonal cycle is attenuated with a factor 10. The approximate time-lag of one and a half month for such a temperature signal is in reasonable agreement with observations. For a signal period of 100 years, we find a time-lag of about 6 years, which is in good agreement with the value by Reid [1991] using a sophisticated multi-level ocean model.

The coupled system behaves quite linear for signal periods larger than two years due to the adopted linear diffusion equations. For smaller periods, the system has a clear interference with the non-linear behaviour of atmospheric radiative transfer. This acts to muffle possible phase resonance in the upper ocean layer. The timescale of atmospheric processes is found to be in the

order of two months. The model acts as a low-pass filter due to the large heat capacity of the ocean.

5.3.3 Model Input

a Greenhouse Gases and Aerosols

The increase of greenhouse gas concentrations as function of time since 1850 has been adopted from the IPCC reports: that is CO₂, CH₄ and N₂O from IPCC, [1990] and CFCs, HCFCs and HFCs from IPCC, [1994]. In order to avoid abrupt changes, we have interpolated the greenhouse gas concentrations at each timestep during the integrations either linearly (N₂O in the period 1850-1900 and CFCs after 1950) or exponentially. The increases of these uniformly mixed greenhouse gases lead to a radiative forcing of about 2.1 Wm⁻². We also account for ozone changes. We assume a linear increase of tropospheric ozone from 1950 up to 8.4 DU in 1990 [Lelieveld and Van Dorland, 1995; Van Dorland et al, 1997, Chapter 4], resulting in a radiative forcing of 0.34 Wm⁻² and a linear decrease of stratospheric ozone since 1970 up to -10.8 DU in 1990 as to fit the estimated radiative forcing of about -0.13 Wm⁻² [WMO, 1992; IPCC, 1995]. The profile changes have been adopted from Shine et al. [1995]. The radiative forcing due to tropospheric sulfate aerosol changes since pre-industrial times have been estimated to amount -0.5 Wm⁻² (direct effect) and about -0.75 Wm⁻² due to changes of cloud optical properties and the potential influence on the lifetimes of clouds (indirect effect). In order to simulate the evolution of tropospheric sulfate aerosols since 1850, we have used the estimate of the sulfate burden as a function of time from IPCC, [1994] together with the radiative forcing of the direct effect, which results in an optical depth increase (at 0.55 μm) of approximately 0.04 for the year 1990. The indirect effect is assumed to be caused totally by a decrease of the modal droplet radius in water clouds, while keeping the liquid water content constant. To match the radiative forcing of -0.75 Wm⁻² in 1990, we compute an average decrease of the radius of about 5%. We did not correct for the 'stack height' in the seventies and eighties [Wigley and Raper, 1992]. Furthermore, we include the effects of stratospheric sulfate aerosols due to volcanic eruptions. Therefore, we adopted the dataset of Sato et al. [1993]. Our model's sensitivity agrees very well with the simple relationship given by Lacis et al. [1992], namely the forcing is approximately equal to -30 Wm⁻² times the stratospheric sulfate aerosol optical depth.

b Solar Activity

We use the dataset of sunspot index (SIDC) for the computation of the solar signals. For the 11-year solar cycle we translate the sunspot index, a measure of the number of sunspots, in terms of a variation of the solar constant. We adopt a change of 0.1% (1.4 Wm⁻²) for a change in sunspot index of 150. This is in agreement with the estimated values by Lean [1991] from observations in the period between 1978 and 1990 (solar cycle 21).

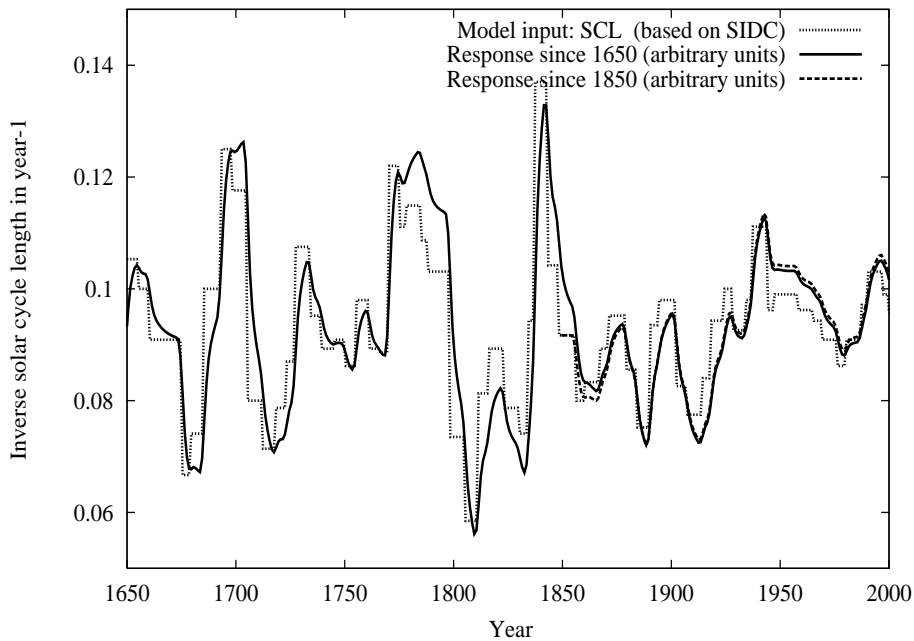


Figure 5.3: Inverse solar cycle length in yr^{-1} from 1650 until 1997 as determined from sunspot minima and maxima (source: SIDC) and subsequent surface temperature response in arbitrary units as computed with the KRCM since 1650 as well as since 1850 (with equal averages in the overlapping period 1850-1997)

The solar cycle length is determined from the position of maxima and minima of sunspot index using the same dataset, given with a resolution of about a month (Figure 5.3). The accuracy is much lower than the resolution due to the large fluctuations during the period of sunspot maxima. The method of computing the solar cycle length from the sunspot maxima and minima introduces a phaseshift of about $3/4$ cycle as the actual length is determined from the full sunspot cycle preceding an extreme value. It should be emphasized though that there is no physical mechanism, which could give an indication of the precise time-lag. Since the system does not possess predictive characteristics, the only condition is that there is a delay. Moreover, we use a statistical method to fit both the amplitude and time-lag. So, the introduction of a possible phaseshift has no relevance for our results. In addition, the modelled climate system show a delay dependent on the signal period (Figure 5.2). Since it is found that the surface temperature response is inversely correlated with the solar cycle length (SCL), we use the solar cycle frequency as a proxy. In order to model the temperature response due to SCL, we have adopted three fictitious mechanisms for which no essential differences with respect to their effects have been found. That is, a change of solar constant, a variation of cloud cover and a change in average cloud droplet size.

5.4 Model Results

5.4.1 Climate Response

We perform time integrations for the changes in atmospheric composition due to human activity since 1850. This is done for the components separately as well as simultaneously. In Figure 5.4 the radiative forcing in terms of equilibrium temperature response, i.e. forcing relative to 1850 times climate sensitivity, and the actual model's surface temperature response are shown for greenhouse gases (well mixed gases and ozone) and for the total effect of sulfate aerosols (i.e. direct and indirect). The actual response is about 70% of the equilibrium value for both components, showing an almost exponential trend in time. In contrast, the response on solar irradiance changes due to the 11-year sunspot cycle reaches about 30% of the equilibrium response (Figure 5.5). These differences can be explained in terms of the amount of heat storage in the ocean for signals with different (dominant) timescales of oscillation (Figure 5.2), implying characteristic attenuation factors and time-lags. Hence, the climate system acts as a low-pass filter, which is demonstrated in Figure 5.3, 5.4 and 5.5: the fine-structure in the forcing disappears in the temperature response. Moreover, the forcing-response relationship appears to be quite linear. Its consequence is twofold: first, we may add the responses due to the various forcing mechanisms. Second, we may scale the amplitude of the response of signals without any defined physical mechanism, retaining the magnitude of their radiative forcings. Some weak non-linear behaviour is found for stratospheric ozone changes resulting in direct local temperature changes due to altered shortwave absorption, because the emitted longwave radiation by greenhouse gases is strongly dependent on stratospheric temperatures. Also, rapid changes in atmospheric composition as compared to the timescale of radiative adjustment in the stratosphere, i.e. about two months, induce non-linear effects. This is the case for large volcanic eruptions as they change the stratospheric aerosol burden in a very short time.

5.4.2 Uncertainties in Climate Response

Although changes of the radiation balance due to increasing levels of uniformly mixed greenhouse gases are relatively well-known (within 15%), large uncertainties do exist for the radiative forcing of tropospheric as well as stratospheric aerosols, especially regarding their indirect effects. Furthermore, the climate sensitivity, which is the translation factor from instantaneous radiative perturbations to final temperature response, ranges from 0.3 to 1.1 K per Wm^{-2} . This introduces a large uncertainty in the attribution of the anthropogenic signal. For instance, if we take these uncertainties into account and correct for the difference between equilibrium and actual response (about 70% as discussed in section 5.4.1), the anthropogenic temperature increase in 1990 ranges from 0.1 K to 1.5 K. This justifies to vary the human signal, preferably through the sulfate aerosol signal, in the statistical optimization procedure. In addition, lack of knowledge on the physical mechanisms, possibly responsible for the effects of solar activity on

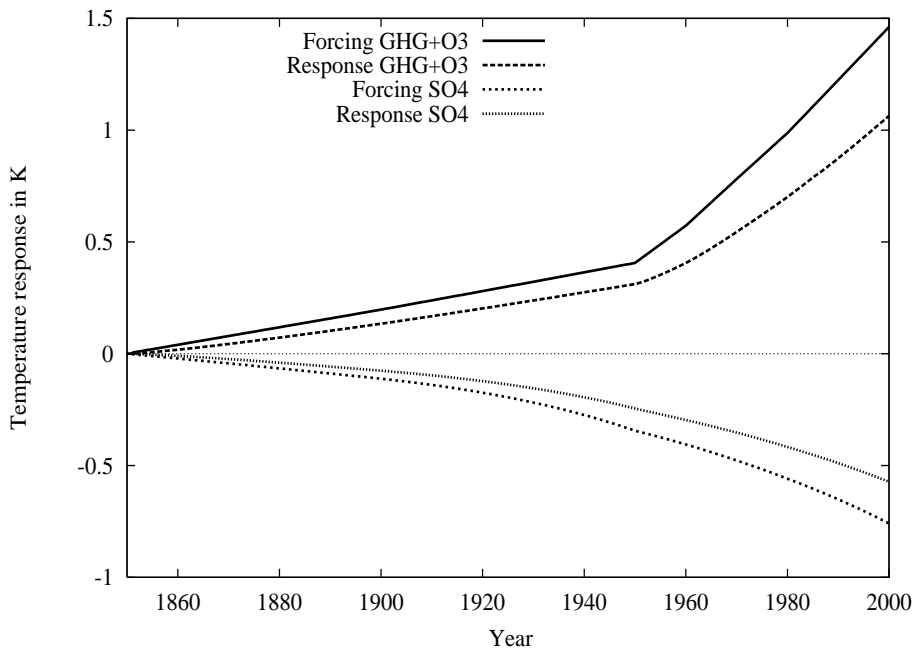


Figure 5.4: Actual surface temperature response and equilibrium response ($\text{forcing} \times \text{climate sensitivity}$) in K for greenhouse gases and sulfate aerosols

climate, hamper model calculations other than in a statistical sense.

Therefore, we optimize the anthropogenic and natural signals, i.e. modelled temperature responses, simultaneously in terms of explained variance. The advantage of this method is that we get amplitude information on the signals, which is not the case for correlation exercises. There are of course restrictions for this method. First, the linearity is essential for such a statistical evaluation. This is approximately the case as shown previously. Second, we may derive the relative contributions of the various forcing mechanisms if their characteristics are orthogonal to a large extent. A measure of orthogonality is given by the correlation coefficient. We have listed these coefficients in Table 5.1 for the anthropogenic, volcanic, and the 11-year as well as the Gleissberg solar signal. The correlation coefficient between the temperature response of greenhouse gases and sulfate aerosols is -0.98 , since they both show an almost exponential trend with opposite signs. Therefore, we cannot separate these signals in the optimization procedure. We may also question the importance of taking the history of climate variations into account. We perform this exercise for the possible climate effects of the Gleissberg signal. In Figure 5.3 we plotted the temperature response (in arbitrary scale) equally determined for two time integrations: starting at 1650 and 1850. If we choose the reference level such that the averages are equal for the overlapping period, no large differences are found. In the optimization procedure we fit

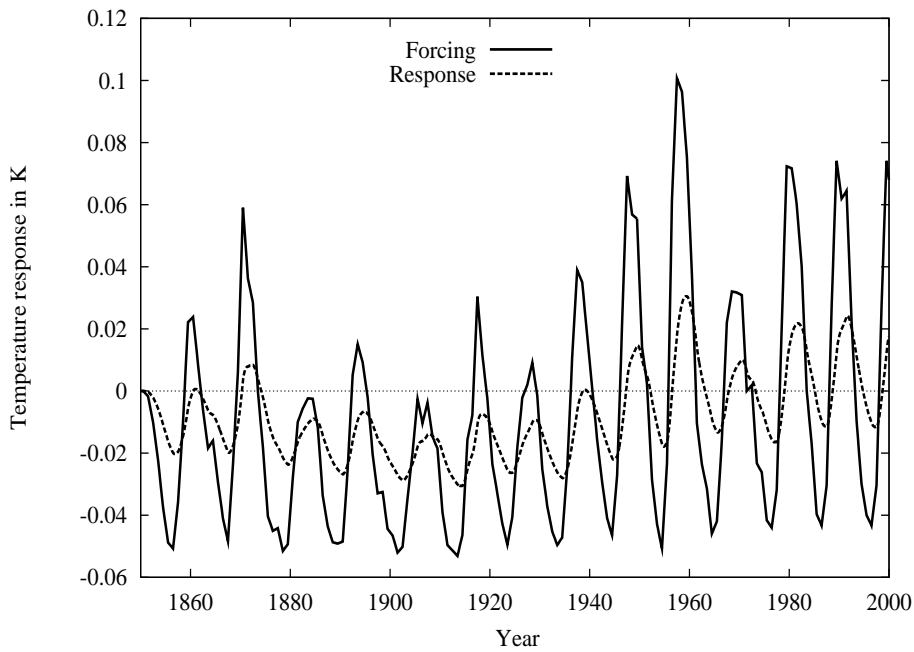


Figure 5.5: Actual surface temperature response and equilibrium response (forcing \times climate sensitivity) in K for the 11-year sunspot cycle

Table 5.1: Correlation matrix for the surface temperature response due to the anthropogenic effect (ANT), greenhouse gases and tropospheric sulfate aerosols, solar cycle length (SCL), 11-year cycle of sunspots (SIN), and volcanic aerosols (VOL), computed with the KRCM for the period 1880-1996. The correlation with the observed surface temperature (OBS) is also given.

	ANT	SCL	SIN	VOL	OBS
ANT	1	0.33	0.53	-0.18	0.72
SCL		1	0.47	0.40	0.70
SIN			1	0.03	0.59
VOL				1	0.12

modelled to observed climate variations, implying that the reference level is of no importance.

Table 5.2: Best fit of global mean surface temperatures, 1880-1996, for the anthropogenic (ANT in K for 1990), solar cycle length (SCL in Wm^{-2} of solar constant change between 1910 and 1940), sunspot cycle (SIN in % of the solar constant for an index change of 150), and volcanic (VOL as a factor of the adopted Sato et al. [1993] dataset) signals. The explained variances are given for the annual mean, 6-year as well as 16-year bicubic spline filtered observed temperature.

ANT	SCL	SIN	VOL	filter	expl.var.(%)
0.41	7.4	—	—	no	76
0.42	7.4	—	—	6-year	87
0.45	6.9	—	—	16-year	90
0.37	7.3	0.14	—	no	76
0.39	7.2	0.11	—	6-year	88
0.43	6.7	0.07	—	16-year	90
0.61	—	—	—	no	56
—	9.9	—	—	no	49
0.59	—	—	0.6	no	62
0.53	—	0.27	0.6	no	64

5.4.3 Statistical Optimization of Temperature Signals

a Anthropogenic and Gleissberg Signal

The anthropogenic as well as the Gleissberg signals vary predominantly on decadal timescales. Greenhouse gases and aerosol burden show both an exponential increase in time (Figure 5.4), while the solar cycle length is characterized by irregular oscillations. In order to fit these signals to observed decadal temperature variations we use a 16-year bicubic spline filter, meaning that the weighting factors for the ± 8 years are zero. The best explained variance of approximately 90% is found for a temperature increase in 1990 relative to 1850 due to anthropogenic influence of 0.45 K and for a solar constant change between 1910 and 1940 of 6.9 Wm^{-2} (Table 5.2). It appears that both signals contribute equally within a few percent to the decadal climate variations, which can be derived from the fact that both signals correlate equally with the observed temperature (Table 5.1). If the solar signal is true, it implies that only 10% of the slow temperature variations is left for internal variability. In case of statistical optimization to the annual mean observed temperature, the explained variance of the sum of both signals decreases from 90% to 76%, again with equal contributions. This suggests that internal variability is dominantly present in the shorter time scales. Only small changes in the amplitude of the signals are found, i.e. 0.41 K for the human effect in 1990 and 7.4 Wm^{-2} for the Gleissberg signal between 1910 and 1940. This is shown in Figure 5.6 as the optimum occurring at the y-axis. If the solar signal does not have any impact on climate, the anthropogenic effect (optimum at 0.61 K in 1990, Table 5.2) explains about 56% of the variance (origin in Figure 5.6). Even if the solar signal would

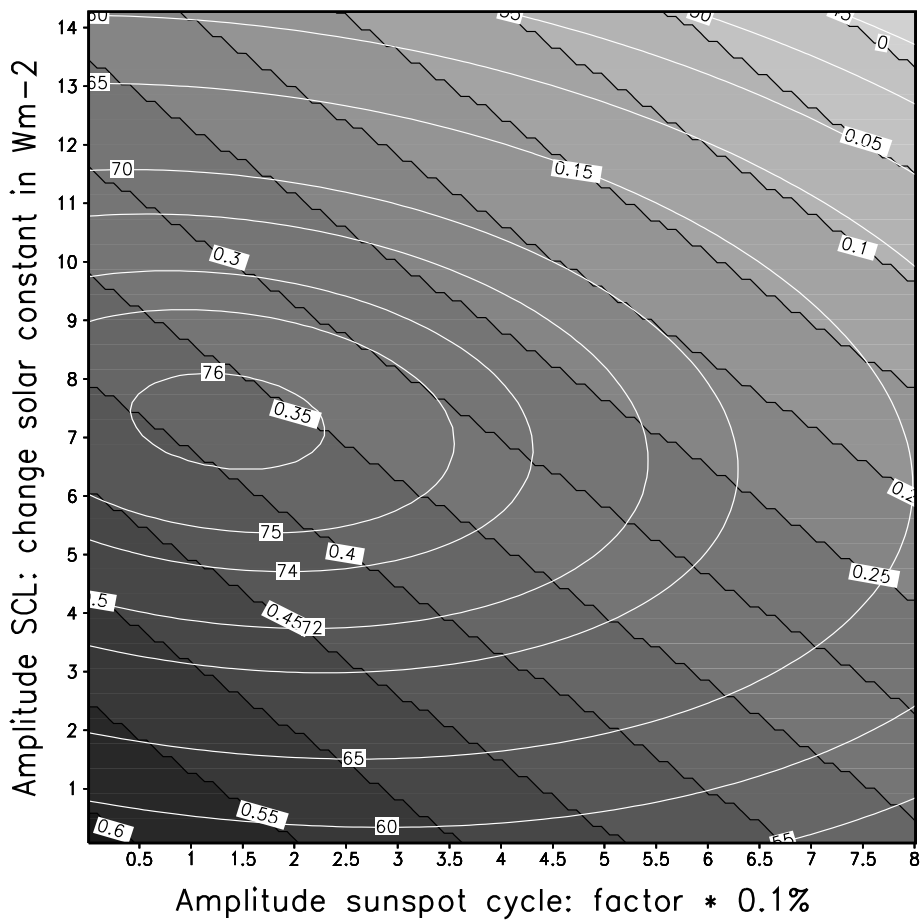


Figure 5.6: Explained variance in % (white contours) of the annual mean observed surface temperature as a function of the anthropogenic effect in K in 1990 (shaded), the solar cycle length signal as an increase of the solar constant in Wm^{-2} between 1910 and 1940, and the 11-year sunspot cycle as a factor relative to the solar constant variation of 0.1% per 150 sunspots

be twice as large as for the best fit (left upper corner, Figure 5.6), the best estimate of the anthropogenic influence in 1990 is still 0.23 K, but the total explained variance drops to the value of 60%. Assuming either no human influence at all or a much larger human influence of 0.9 K (1990 value), the explained variance is less than 50%. Combination of both signals for the best fit results in differences with the observed (filtered) temperature of less than ± 0.1 K. Assuming no anthropogenic influence, we find large differences especially for the period after 1970. This indicates that the rapid temperature increase of the last three decades cannot be explained with the Gleissberg signal.

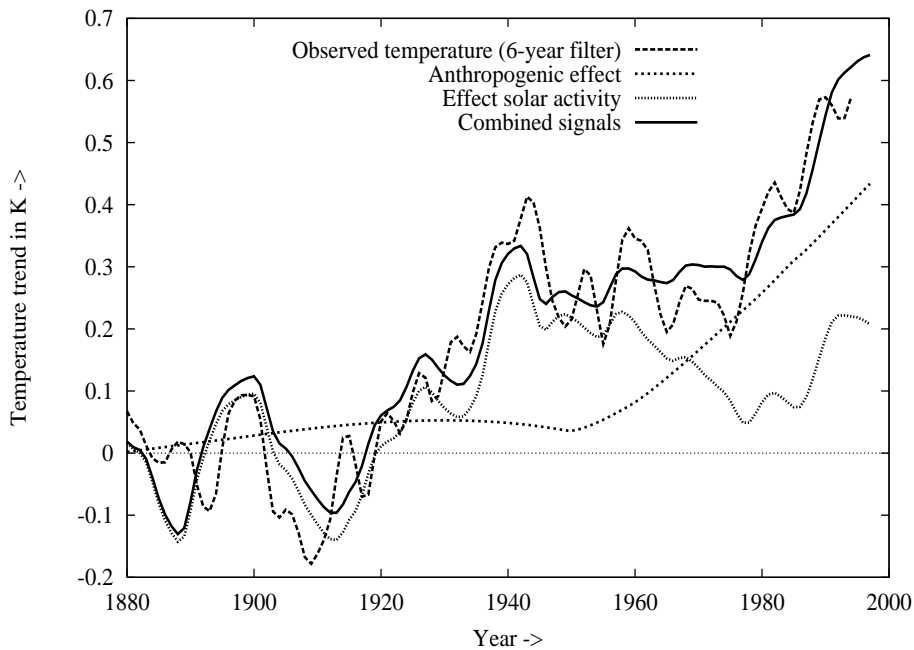


Figure 5.7: Best fit of the computed surface temperature response for the anthropogenic effect (dashed line), the solar effect combined from the 11-year cycle and the Gleissberg signal (dotted line), the sum of these signals (solid line) and the (6-year) filtered observed temperature (heavy dashed line)

b Anthropogenic, Sunspot and Gleissberg Signal

We perform the statistical optimization procedure for the anthropogenic and both solar signals, the 11-year sunspot and the Gleissberg cycle, simultaneously (Figure 5.6). The total explained variance of the annual mean observed temperature is about 76%. Filtering improves this value (Table 5.2), but since the 11-year solar signal is involved, we should avoid using filters which passes through very low frequency characteristics only. Using a 6-year bicubic spline filter, we find a total explained variance of 88%. The division over the three signals is as follows: 40% for the anthropogenic influence as well as the Gleissberg cycle and only 8% can be attributed to the sunspot cycle. In terms of amplitude this is about 0.4 K for the human effect in 1990, 7.2 Wm^{-2} for the solar constant in the SCL signal between 1910 and 1940, and 0.11% change of solar constant for a sunspot number change of 150. The latter is in good agreement with satellite measurements [Lean, 1991]. Combination of the two solar signals and the anthropogenic influence of the best fit, result in a temperature record which agrees very well with the observed temperature (Figure 5.7). The 11-year sunspot cycle response is an order of magnitude smaller than the anthropogenic and Gleissberg signal, but its trend acts to decrease the difference with

the observed temperature as compared to the results of section 5.4.3.a., especially in the period 1940-1970. In Figure 5.8 the total response of the best fit is plotted as a function of altitude and depth. In the troposphere the temperature variations are of the same order as at the surface (Figure 5.7) due to the strong coupling. In the ocean the signal is attenuated and delayed, especially in the deeper layers. The stratosphere cools mainly due to enhanced emission of CO₂ in the strong 15 μm band, hence caused by human activity. In addition, the excessive cooling of the lower stratosphere since the seventies is caused by the trend in ozone depletion and matches the observed temperature changes of $-0.4 \pm 0.12^\circ\text{C}/\text{decade}$ [Oort and Liu, 1993] quite well. The strong surface temperature increase in the last two decades can be attributed largely to the industrial activities of mankind.

c Sunspot and Gleissberg Signal

In case of fitting both solar signals to the observed temperature, the residue shows a clear increase after 1970, which matches best with an anthropogenic effect of 0.26 K in 1990. In this case, the contribution of the sunspot cycle is a factor 5 larger, while hardly any change is found for the Gleissberg signal. We may derive this point from Figure 5.6. This implies that no combination of the solar signals can be found to explain the rapid increase of global mean temperature since 1970.

d Anthropogenic and Volcanic Signal

We may question whether the combination of human and volcanic activity could account for the observed temperature variations of the last century. Particularly, the absence of large volcanic eruptions in the period between 1920 and 1960 is likely to induce a warming. If we optimize both signals statistically, the best fit in terms of explained variance (62%) occurs for a human induced warming in 1990 of 0.59 K and a volcanic effect (Table 5.2, Figure 5.9), which is about 60% of the computed response using the database of Sato *et al.* [1993]. This discrepancy might be (partly) caused by the climate sensitivity of the KRCM or by secondary (warming) effects after the negative forcing due to increased stratospheric aerosol burden. We may conclude from Figure 5.9 that the combination of human and volcanic activity cannot account for the cool period in 1910 and the warm period in 1940. Nevertheless, the absence of clear decadal trends due to volcanic aerosols does not imply that individual large eruptions cannot have large impacts on global mean surface temperature.

5.5 Discussion and Conclusion

In this paper we investigate the role of anthropogenic and natural radiative forcing mechanisms using a 1D ocean-atmosphere model. Statistical evidence is put forward to estimate the amplitude of the potential solar effects on decadal time scales. Although the physical mechanism for

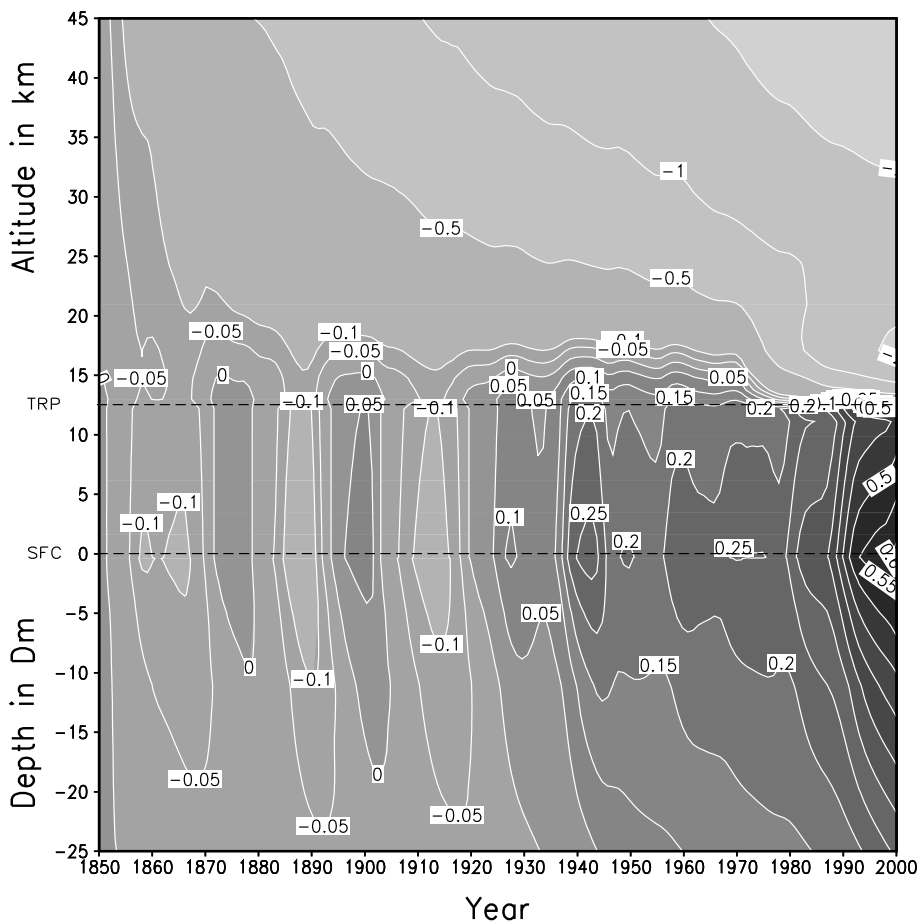


Figure 5.8: Computed temperature response as a function of time and altitude (as well as depth) for the best fit of surface temperature using the anthropogenic effect (well-mixed greenhouse gases, ozone and sulfate aerosol) and the solar effect combined from the 11-year cycle and the Gleissberg signal

the human influence, both the enhanced greenhouse effect [Van Dorland, 1997, Chapter 4] and the cooling due sulfate aerosols, is well understood in terms of their perturbations on the radiation balance and the subsequent climate changes, the amplitude of this signal is highly uncertain. In terms of radiative forcing the sulfate aerosol direct and indirect effects contribute most to this uncertainty. The translation of total anthropogenic radiative forcing to final (equilibrium) climate response cannot be estimated very accurately either, because feedback mechanisms in the climate system have not been modelled unequivocally. The partition of heat storage in the oceans and direct heat release into the atmosphere through longwave radiation and convective processes, introduces some uncertainty in the ratio of actual and equilibrium response. Taking

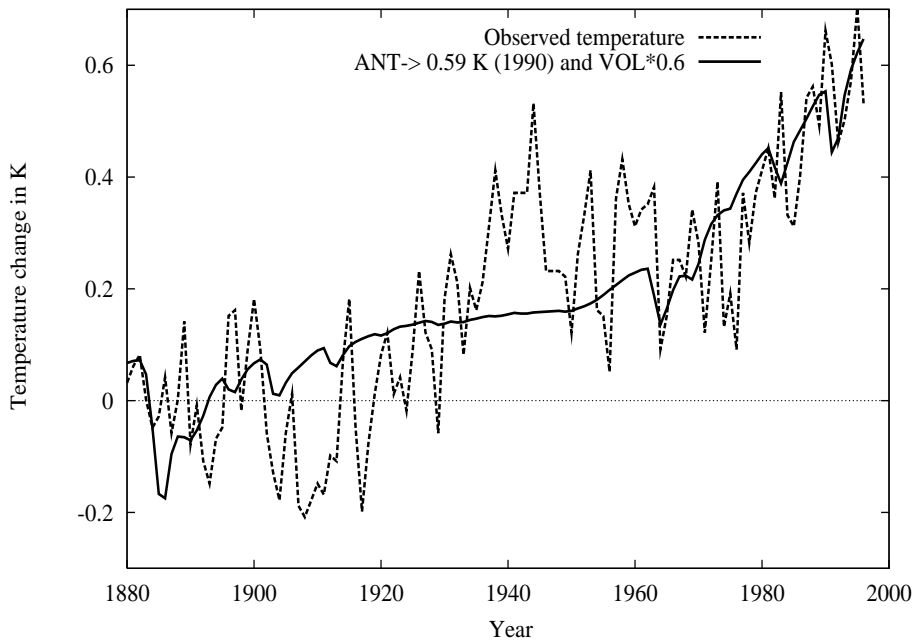


Figure 5.9: Best fit of the computed surface temperature response for the anthropogenic effect combined with the volcanic activity response (solid line) and the annual mean observed surface temperature (dashed line)

these uncertainties into account results in an anthropogenic signal in 1990 ranging from 0.1 to 1.5 K.

Therefore we optimize the anthropogenic and (potential) natural signals simultaneously with respect to the explained variance of the observed temperature in the period 1880-1996. Since we found that the volcanic signal does not contribute significantly to the explained variance, optimization has been performed with the anthropogenic and solar signals. In this case, we use a 6-year bicubic spline filter in order to smooth the year-to-year variations in the observed temperature. We find that about 88% of the global mean temperature variations since 1880 can be attributed to human influence (40%), to the Gleissberg signal (40%), and to the 11-year sunspot cycle (8%). The concurrent variation of the solar constant over a sunspot cycle is found to be about 0.11% (1.5 Wm^{-2}) per sunspot index difference of 150, which is in reasonable agreement with measurements [Lean, 1991]. In contrast, the impact of the Gleissberg signal is not based on a physical mechanism, but appears as a purely statistical correlation. Its magnitude can be translated in terms of a solar constant variation of about 0.5% between the (relative) minimum in 1910 and maximum in 1940. Other possibilities giving the same response are (average) cloud cover variations of 2% or average droplet (not ice crystals!) variations of 10%. There are no

measurements to support either one or a combination of these possible mechanisms, but the magnitude of these variations may be considered as not beyond reality in principle [Zhang *et al.*, 1994; Hoyt and Schatten, 1993]. For this optimum in explained variance we compute a temperature increase of 0.4 K due to the human influence in 1990 relative to 1850, the end of the pre-industrial era. Variation of the potential climate effects of the solar cycle length from zero to twice the optimum value result in best fits for the anthropogenic trends in 1990 of 0.6 K and 0.2 K, respectively. Hence, statistically we may limit the human influence in 1990 at 0.4 ± 0.2 K. It must be emphasized though that we may not be able to narrow the uncertainty of future projections due to the enhanced greenhouse effect substantially, because the ranges in radiative forcing as well as climate sensitivity remain.

The fact that the investigated mechanisms are orthogonal to a large extent (otherwise statistical evaluation would be impossible) justifies the separation of characteristic effects in the past century: that is a temperature increase between 1910 and 1940 due to the Gleissberg signal, the slight cooling between 1940 and 1970 due to the combination of cooling by the Gleissberg signal partly compensated by the human influence, and the rapid anthropogenic warming since 1980 (Figure 5.7). The sunspot cycle signal, which is an order of magnitude weaker than the Gleissberg signal acts to improve the fit between 1940 and 1970. In contrast to the anthropogenic influence, which is an almost exponential signal in time, the potential climate effects of the solar cycle length as well as the sunspot cycle show fluctuations in time. For such quasi-periodic signals, we should distinguish between the amplitude of variability and the actual trend at a certain moment. The actual trend for the combined solar signal in 1990 as compared to the average over the period 1856-1900 is about 0.2 K. This is only marginally larger than, and within the uncertainty range of the most recent IPCC estimates of the solar influence [IPCC, 1995]. Therefore, the investigated impact due to solar activity hardly affects the IPCC conclusions concerning the anthropogenic signal. Instead, the suggested amplitude of the Gleissberg signal is competitive with the internal variability of the climate system. This internal variability appears as noise with a certain amplitude in a range of timescales, which makes observed climate anomalies acceptable, rather than accounting for an exact match of warmer and cooler periods.

Combining the anthropogenic and volcanic signals results in a much lower total explained variance of the observed temperature than the combinations in which the solar activity is included as described above. It should also be emphasized that no combination of sunspot cycle and long-term solar variation can explain the rapid increase of global mean temperature since 1970. This is in contrast with the work of Friis-Christensen and Lassen [1991].

We have also tested the cosmic ray - cloud cover hypothesis of Svensmark and Friis-Christensen [1997], in which they claim a large impact of the sunspot cycle on global temperatures. They found a high correlation between cloud cover and cosmic ray intensity over about one cycle, which in turn is inversely connected with the number of sunspots. The impact of the suggested changes in cloud cover on the global temperatures is shown in Figure 5.10. Although some of the observed 11-year temperature fluctuations match the computed effects of the sunspot cycle,

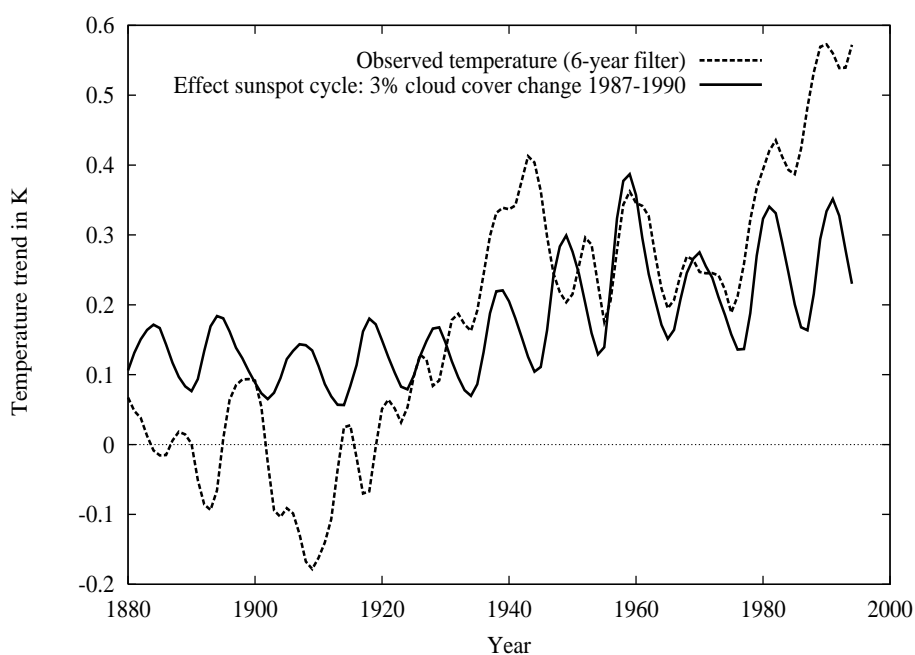


Figure 5.10: Test of the cosmic ray - cloud hypothesis of Svensmark and Friis-Christensen [1997]. A decrease of 3% in average cloud cover is adopted between the minimum (1987) and maximum (1990) solar activity of cycle 22, resulting in a radiative forcing of 1.25 Wm^{-2} . This concept is proportionally applied to the number of sunspots since 1880

this solar signal is out of phase before 1950. Moreover, the observed long-term trends are considerably larger, showing a much colder epoch before 1930, and warmer epochs around 1940 as well as in the last two decades. Thus the proposed mechanism, explaining about 38% of the variance, has a poor performance.

In the absence of a physical mechanism for the climate effects of solar cycle length variations, and hence causality, we may conclude on basis of the found correlation with the observed temperature that there is a possible impact on climate. This signal would reduce the estimated internal variability of the climate system, rather than the anthropogenic influence, which is also physically well-understood.

acknowledgments We thank the providers of the temperature data, P.D. Jones, and sunspot indices (SIDC). We acknowledge Piet Stammes and Bert Holtslag for reading the manuscript.

Chapter 6

Summary and Outlook

6.1 Summary

In this dissertation we focus on atmospheric radiative transfer and its change in the past one-and-a-half century. In this period the composition of the atmosphere has been significantly changing due to human activities. Therefore, we use a radiative transfer scheme, in which we incorporate all relevant constituents for climate studies. We evaluate this scheme with surface measurements of the downward longwave flux. In addition, we construct a 1D coupled ocean-atmosphere model, in which the radiative transfer scheme forms a crucial part. Furthermore, we apply these models to calculate the radiative forcing and subsequent temperature responses due to a variety of anthropogenic and natural forcing mechanisms.

Our motive for this approach is that on global scale perturbations of the radiation balance are strongly linked with subsequent (equilibrium) surface temperature changes, although the conversion factor, the so-called climate sensitivity, contains an uncertainty by a factor of three among the present generation of 3D climate models. This implies that an estimate of the climate effects due to forcing mechanisms can only be obtained in a relative sense by studying the radiative perturbations. Moreover, this justifies the use of a 1D climate model, i.e. a radiative-convective model coupled with a simple ocean model, to study first order transient climate effects of forcing mechanisms [IPCC, 1997]. Such an approach is very useful when comparing model output with observed temperature changes.

Overview of Main Subjects

A broad-band radiative transfer scheme, which is based on the original *Morcrette* [1991] longwave and *Fouquart and Bonnel* [1980] shortwave schemes, has been further developed with respect to the inclusion of several greenhouse gases such as CH₄, N₂O, CFCs, HCFCs and HFCs, as well as the implementation of the 14 μm band of ozone and a new formulation of the water vapor continuum (Chapter 3). Furthermore, we equipped the scheme with optical parameters of eleven aerosol components, based on the Global Aerosol Data Set (GADS) [Koepke *et al.*, 1996]. The extended radiative transfer scheme has been selected to be part of the ECHAM4 climate model [Roeckner *et al.*, 1996]. We have evaluated the longwave radiative transfer scheme with surface measurements of the downward radiation at Cabauw, the Netherlands, under clear sky conditions. In this evaluation, the scheme has been tested for three compilations of spec-

trosopic line parameters. These parameters form the basis of pre-calculated temperature and pressure dependent coefficients of the transmission functions for the greenhouse gases used in the broad band scheme. These pre-calculations are performed with a detailed (narrow band) longwave radiative transfer scheme. Also, we examined the impact of a change of the water vapor continuum formulation. The sensitivity to possible inaccuracies in the input profiles of temperature, humidity and ozone has been studied and compared with the standard deviation and bias between the measurements and observations.

Qualitative insight in (tropospheric) longwave radiative transfer is obtained by simplifying the governing radiative transfer equation into an analytical model, having three-parameters (Chapter 2). The validity of this approximative model is illustrated by comparing its qualitative results for the flux profile in the clear sky part of the global and annual mean atmosphere with calculations using the aforementioned broad band scheme. In addition, the mechanism of the enhanced greenhouse effect is discussed with the help of this analytical model. The effect is separated for gases which are radiatively active inside and outside the most transparent part of the longwave spectral region.

The broad band radiative transfer scheme is further used to compute global patterns of radiative forcing due to increases of tropospheric ozone and sulfate as well as nitrate aerosols (Chapter 4). These constituents possess the largest uncertainty ranges with respect to their radiative forcings by which the total anthropogenic forcing is not well-known. The concentration fields of these short-lived constituents and their precursors on a $10^{\circ} \times 10^{\circ}$ grid are computed with a three-dimensional transport/chemistry model of the atmosphere (MOGUNTIA) for the preindustrial (1850) case, the contemporary case (1990) and for the future (2050). The longwave as well as the shortwave sensitivities of ozone are examined so as to estimate the uncertainty range of the computed radiative forcing. In addition, analytical fits are derived for the shortwave forcing by tropospheric ozone and sulfate aerosol as a function of surface albedo and the solar zenith angle.

The broad band radiative transfer scheme is incorporated in a 1D coupled ocean-atmosphere climate model (Chapter 5). In this model, we account for the fast redistribution of energy due to sensible and latent heat fluxes, which maintain an average tropospheric lapse rate of 6.5 K/km. In the model heat is stored in the ocean, thereby delaying and attenuating the response as compared to the equilibrium response on forcing mechanisms. We also account for the water vapor feedback in our climate simulations. The climate model is tuned as much as possible towards the presently observed global mean climatology. With this model the temperature responses on several natural and anthropogenic forcing mechanisms are examined. For the anthropogenic component we use the time evolution of greenhouse gases and sulfate aerosols since 1850. The effects of stratospheric aerosol changes due to (large) volcanic eruptions and of a possible impact of variations in solar activity are incorporated so as to study the role of natural forcing mechanisms. We note that there is large uncertainty in the total radiative forcing due to human activity, mainly through the effects of anthropogenic aerosols. In addition, the physical mech-

anism of the solar forcing is not (well) known. Therefore, we use a statistical technique to fit the sum of the anthropogenic and natural climate responses to the observed global mean temperature [Jones, 1994]. As such we aim to estimate their possible relative contributions to the observed global warming.

Overview of Main Conclusions

1. Increases of greenhouse gases result in an increased opacity of the atmosphere for infrared radiation, except in the saturated part of the spectrum. Its consequence is a reduction of the upward longwave flux and an increase of the downward flux at the tropopause level, both contributing to a positive radiative forcing. For gases active in the atmospheric window region, this reduction of the upward flux originates from increased attenuation of the emitted longwave radiation from the earth's surface. In contrast, for greenhouse gases active outside the window region, e.g. where most of the CO₂ bands are located, the flux reduction at the tropopause is mainly caused by changes in radiation originating from the atmosphere itself. Such a change in atmospheric flux results from a change in the cascade of enhanced absorption and emission, which occurs if the longwave opacity of the atmosphere is increased.

2. Saturation occurs in a narrow spectral region in the center of the 15 μm CO₂ band. It implies that up to a certain altitude (in the stratosphere), where CO₂ densities are high enough, changes in the mixing ratio of this greenhouse gas do not result in net flux changes. Therefore, its radiative forcing in this narrow spectral region is close to zero. However, the unsaturated wings of the 15 μm band are strong enough to dominate in the total radiative forcing due to CO₂ changes by about 90%.

3. The changes in radiative fluxes at the atmospheric boundaries due to increases of greenhouse gases can be interpreted as upward radiation which is effectively emitted from a higher altitude (on average in the troposphere where temperatures are lower), and downward radiation which is effectively emitted from a lower level, which is on average close to the earth's surface. From this point of view it follows that the average decrease of temperature with altitude in the troposphere is essential for the occurrence of the enhanced greenhouse effect. This conclusion is confirmed by our simplified analytical approach of longwave radiative transfer. The balance at the top of the atmosphere, which is disturbed by less outgoing infrared radiation as compared to the net incoming solar radiation, is eventually restored by an increase of the temperature of the surface and the troposphere, thereby increasing the outgoing longwave radiation. This is known as the enhanced greenhouse effect.

4. The broad band radiative transfer scheme, used throughout this dissertation, compares very well with observations of the downward flux at the surface for a large range of temperatures and humidities in 253 clear sky cases. Using the HITRAN 1996 compilation of spectroscopic

parameters and the water vapor continuum formulation of *Giorgetta and Wild* [1995], we find a correlation of 0.99. The bias of only -2 Wm^{-2} and the standard deviation of 4.2 Wm^{-2} are both within the range of measurement errors. Using other compilations of spectroscopic line parameters, the differences between modelled downward radiation and the measurements still remain smaller than the measurement errors. Therefore, improvement can be accomplished by increasing the spectral resolution as well as improving the water vapor continuum formulation in broad band radiation schemes for climate modelling purposes. The agreement between our model and the measurements is good enough to be confident in the accuracy of the radiative forcing calculations, performed in the context of this dissertation.

5. We find globally and annually averaged radiative forcings over the industrial period (1850–1990) of $+0.38$ and -0.36 Wm^{-2} for increases in tropospheric ozone and sulfate aerosol (direct effects), respectively. These values indicate an approximate balance, which is also due to the fact that both constituents are confined to specific regions, since their atmospheric residence times are relatively short, albeit that ozone changes are more zonally dispersed. However, both constituents have characteristic seasonal cycles, and their forcing dependencies on several radiative parameters are quite different, resulting in large seasonal and regional differences between their radiative forcing patterns. By examining the longwave as well as the shortwave sensitivities in relation to the uncertainties in the model-calculated fields and atmospheric conditions, we find an estimate of the uncertainty range in the radiative forcing due to tropospheric ozone increases of about 40%. Adding the radiative forcing due to well-mixed greenhouse gases since 1850 to that of ozone and sulfate aerosols, some industrial regions show a net negative forcing, indicating that the cooling effects of aerosols dominate. In the northern hemisphere we find the largest longitudinal gradients in the total radiative forcing due to human activities (excluding indirect effects of aerosols and stratospheric ozone depletion) in the summer season, especially in the coastal regions. This poses some questions about possible consequences for climate on regional scale due to dynamical feedbacks.

6. We made a first estimate of the radiative forcing due to nitrate aerosols, which tend to be one order of magnitude smaller than the forcing due to sulfate aerosols on a global scale. However, in some regions in Europe and the United States, large negative values of its radiative forcing have been found. Also, we made an estimate of the radiative forcing due to ozone and sulfate aerosol increases for the future (1990-2050). We demonstrated that a shift of the regions with the largest forcings (positive for ozone and negative for sulfate aerosols) towards countries with emerging economies can be expected.

7. We derived analytical fits for the (shortwave) forcing due to changes in sulfate aerosol as well as ozone, as a function of surface albedo and solar zenith angle. Our fit for sulfate aerosols performs better than the relationship by *Charlson et al.* [1991] in which the surface albedo is the only parameter. These analytical expressions are useful in 3D models, for which the implementation of a sophisticated radiation model is too time expensive.

8. We tested the cosmic ray – cloud cover hypothesis of *Svensmark and Friis-Christensen* [1997], which proposes a large impact of the sunspot cycle on global temperatures. Although some of the observed 11-year temperature fluctuations match the computed effects of the sunspot cycle, this solar signal is out-of-phase with the temperature record before 1950. Moreover, the observed long-term trends are considerably larger, while the 11-year temperature fluctuations are generally much smaller than can be expected from the suggested cloud cover variations. Instead, we find that the observed 11-year temperature variations correspond best with a 0.11% change in the solar constant per sunspot index difference of 150, which is in reasonable agreement with measurements [*Lean*, 1991].

9. The suggested dominant influence of long-term variations in solar activity [*Friis-Christensen and Lassen*, 1991], the so-called Gleissberg cycle, has also been examined. We find that this signal might be responsible for the observed temperature increase between 1910 and 1940, and partially responsible for the slight cooling between 1940 and 1970. However, the rapid temperature increase of the last two decades is likely to originate from anthropogenic emissions. Therefore, the Gleissberg cycle, for which we lack any physical mechanism with respect to its climate impact, is more competitive with the internal variability of the climate system than with the anthropogenic influence. We find that 88% of the slightly smoothed observed temperature variations are explained for a combination of the anthropogenic influence (40%), the 11-year sunspot cycle (8%) and the Gleissberg cycle (40%).

10. We estimate from the calculated climate response to anthropogenic and natural forcing mechanisms and comparison with the observed global and annual mean surface temperature since 1856, that the human influence on the latter up to now is $+0.4 \pm 0.2$ K.

11. Simulations with our 1D climate model show stratospheric cooling due to enhanced emission of mainly CO₂ in the 15 μ m band, hence caused by human activity. In addition, the model reproduces the excessive cooling in the lower stratosphere since the seventies, which is caused by the trend in ozone depletion [*Van Dorland and Fortuin*, 1994] and matches the observed temperature changes of -0.4 ± 0.12 K per decade [*Oort and Liu*, 1993] quite well.

6.2 Outlook

The science of climate change has grown into a multidisciplinary field of research. The general motive of putting much effort world-wide in climate research is primary driven by the notion that we face a risk of rapid global warming in the next century, which is expected to be more pronounced than the speed of natural variations since the end of the last ice-age about 12,000 years ago. The increase of global mean near surface air temperatures in the last two decades certainly fits into this picture, but unequivocal proof that this is caused by human activities cannot be given. Therefore, there is debate on the relative roles of anthropogenically and naturally induced climate change, which is called the attribution problem [*IPCC*, 1995].

In some cases, criticism results in complete negation of the human influence on climate [ESEF, 1996]. In this dissertation we have discussed two controversies, namely the subject of CO₂ saturation in relation to the misinterpretation of the mechanism of the enhanced greenhouse effect [Barrett, 1995] (see Chapter 2) and the suggested dominant climate effects of variations in solar activity [Friis-Christensen and Lassen, 1991; Svensmark and Friis-Christensen, 1997] (see Chapter 5). Since the issue of climate has been placed on the political agenda, such controversies lead quite frequently to doubts about the usefulness of reducing greenhouse gas emissions.

We may pose the fundamental question at what stage we will have gathered enough evidence to prove that human activities cause global warming. By the time we know the answer, it is without any doubt too late for taking measures due to the following reasons: Firstly, unequivocal proof of the enhanced greenhouse effect means that the amplitude of the warming signal must be about one order of magnitude larger than the estimated climate variability from observations and the upper limit of possible external forcing mechanisms. Climate variability is of the order of 0.5 K in the past century. Secondly, due to the long residence times of most greenhouse gases the warming will continue for at least one century [IPCC, 1995].

For the time being, we have to rely on our knowledge of the physics of the climate system, which is far from complete. However, since on a global scale perturbations in the radiation balance are linked with temperature changes, the radiative forcing due to anthropogenic greenhouse gases and aerosols can be compared with that by other mechanisms, such as variations in the solar constant, changes in the stratospheric aerosol content due to volcanic eruptions, and surface albedo changes. The radiative forcing due to increases of uniformly mixed greenhouse gases (CO₂, CH₄, N₂O, CFCs, HCFCs and HFCs) since pre-industrial times is relatively well-known (within 15%) and estimated to be about +2.5 Wm⁻². CO₂ contributes most with about 60%. The radiative effects of ozone changes, i.e. tropospheric increases and stratospheric decreases, are more uncertain with a radiative forcing of +0.38±0.15 Wm⁻² (Chapter 4) and -0.05 to -0.2 Wm⁻² [IPCC, 1995], respectively. In contrast, the radiative perturbations due to aerosols are poorly known. Recent estimates of the direct effects yield a negative forcing of -0.5 Wm⁻² with a factor of two uncertainty. The indirect effects of aerosols, i.e. changing the optical properties and lifetimes of clouds, have a very low confidence level. The forcing lies somewhere between the 0 and -1.5 Wm⁻². This results in a total anthropogenic radiative forcing of +1.5±1.0 Wm⁻². Figure 6.1 shows the radiative forcing due to changes in greenhouse gases, sulfate aerosols and the total anthropogenic forcing added to the effects of large volcanic eruptions as calculated with the radiative transfer scheme [Van Dorland, 1998]. The latter curve shows that large volcanic eruptions have a dominant impact on short time scales. In contrast, human activities cause a steady increase of the total radiative forcing, in particular since 1970. This picture is in general agreement with the observed global mean temperature increase with an approximate delay of a decade due to the heat capacity of the world's oceans (Chapter 5).

Based on future emission scenarios, it is expected that effects of greenhouse gases will dominate over the cooling effects of aerosols in the next century. This results in a total radiative

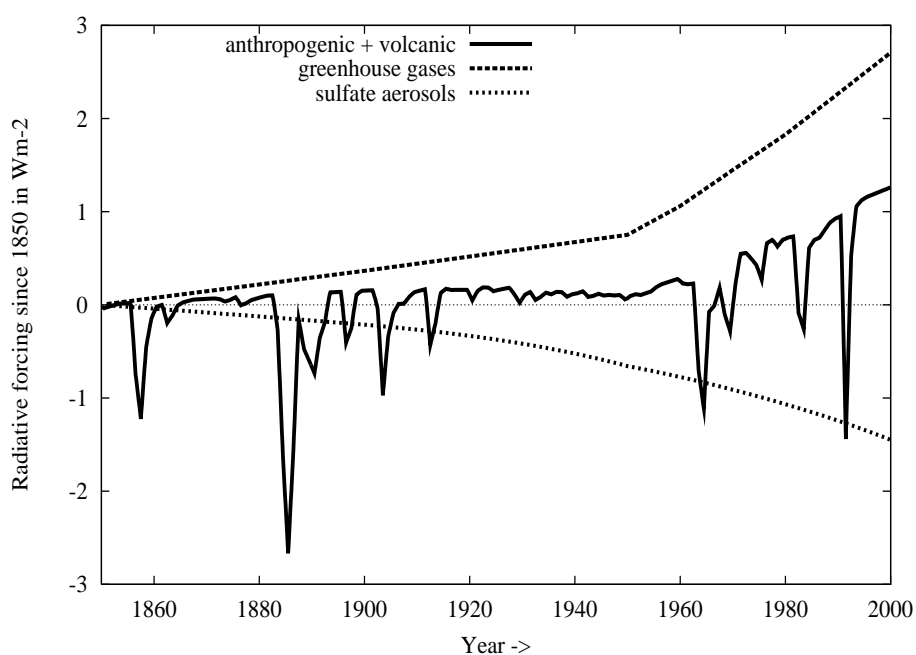


Figure 6.1: Estimate of the radiative forcing in Wm^{-2} since 1850 due to increases of the greenhouse gases CO_2 , CH_4 , N_2O , CFCs and tropospheric ozone increases as well as depletion of stratospheric ozone (curve 'greenhouse gases'), direct and indirect effects of sulfate aerosols (curve 'sulfate aerosols'). The radiative forcing due to changes of volcanic aerosol in the stratosphere [Sato et al., 1993] is added to the total anthropogenic forcing of greenhouse gases and aerosols (curve 'anthropogenic + volcanic'). These curves are calculated with the broad band radiative transfer scheme using global and annual average atmospheric conditions.

forcing of +4 to +8 Wm^{-2} in 2100 [IPCC, 1995]. It should be emphasized that present uncertainties of the total radiative forcing are excluded in this range. Adopting these uncertainties, the total radiative forcing in 2100 will amount somewhere between +1.5 and +13 Wm^{-2} . Using the uncertainty in climate sensitivity, being a factor of three (see Chapter 2), the possible global mean near surface air temperature increase ranges from +0.5 K to +14 K. The lower limit is approximately equal to the estimated climate variability in the last century. The upper limit would exceed natural climate variations since the end of the last ice-age by a factor of seven (see section 2.6.2)! Moreover, from climate simulations with complex 3D models it follows that temperature increases due to the enhanced greenhouse effect are unequally distributed over the globe. Therefore, we face a serious risk of effects associated with climate change due to human activity in the next century even without the possible unpleasant surprises due to nonlinear climate feedbacks.

But how realistic are both aforementioned limits of the global mean temperature increase? Since the product of radiative forcing and climate sensitivity determines the global mean temperature change, observations of temperature in the next decades will contain some information about the bounds of these parameters. In fact, we based our estimate of the total human influence on climate up to now, namely between 0.2 and 0.6 K (see conclusion 10), on the comparison with the observed temperature. Simultaneously, it is likely that additional information about anthropogenically induced climate change will be extracted from a combination of model output and observations of changes in the temperature patterns, the so-called fingerprint method [Santer *et al.*, 1996].

Nevertheless, efforts should be put in narrowing the uncertainty ranges of the radiative forcing due to the direct and indirect effects of aerosols. Furthermore, understanding of changes in the hydrological cycle and in particular the role of clouds therein, are crucial for the determination of the magnitude of the climate sensitivity parameter. Also, the indirect effects of aerosols are tightly connected with the microphysics of clouds. In this respect, global satellite monitoring together with the development of accurate retrieval algorithms for ozone, aerosols and clouds are expected to improve climate modelling.

Although comprehensive 3D coupled ocean-atmosphere models are necessary to study and understand climate cycles and feedback mechanisms, radiative transfer schemes and simple 1D climate models remain useful tools for the determination of the radiative forcing and the subsequent global and annual mean temperature response due to anthropogenic and natural forcing mechanisms.

References

- AFEAS (Alternative Fluorocarbon Environmental Acceptability Study), *Scientific assessment of stratospheric ozone*, volume II, appendix, WMO/UNEP rep., Washington DC, USA, 1989.
- d'Almeida, G.A., P. Koepke and E.P. Shettle *Atmospheric Aerosols Global Climatology and Radiative Characteristics*, 562 pp., A. Deepak Publ., Hampton, Va., USA, 1991.
- Barrett, J., The roles of carbon dioxide and water vapour in warming and cooling the Earth's troposphere *Spectrochimica acta*, 51A, 415-417, 1995.
- Benkovitz, C.M., M.T. Scholtz, J. Pacyna, L. Tarrason, J. Dignon, E.C. Voldner, P.A. Spiro, J.A. Logan, and T.E. Graedel, Global gridded inventories of anthropogenic emissions of sulfur and nitrogen, *J. Geophys. Res.*, 101, 29239-29253, 1996.
- Boucher, O., and T.L. Anderson, General circulation model assessment of the sensitivity of direct climate forcing by anthropogenic sulfate aerosols to aerosol size and chemistry, *J. Geophys. Res.*, 100, 26117-26134, 1995.
- Brezinski, C., Convergence acceleration methods: The past decade, *J. Comput. Appl. Math.*, 12-13, 16-39, 1985.
- Callendar, G.S., The artificial production of carbon dioxide and its influence on temperature, *Quart. J. Roy. Met. Soc.*, 64, 223-237, 1938.
- Cess, R.D., D.P. Kratz, S.J. Kim and J.Caldwell, Infrared radiation models for atmospheric methane, *J. Geophys. Res.*, 91, 9857-9864, 1986.
- Cess, R.D, M.-H. Zhang, P. Minnis, L. Corsetti, E.G. Dutton, B.W. Forgan, D.P. Garber, W.L. Gates, J.J. Hack, E.F. Harrison, X. Jing, J.T. Kiehl, C.N. Long, J.-J. Morcrette, G.L. Potter, V. Ramanathan, B. Subasilar, C.H. Whitlock, D.F. Young, Y. Zhou, Absorption of solar radiation by clouds: observations versus models, *Science*, 267, 496-499, 1995.
- Charlson, R.J., J. Langner, H. Rodhe, C.B. Leovy, and S.G. Warren, Perturbation of the northern hemisphere radiative balance by backscattering from anthropogenic sulfate aerosols, *Tellus*, 43AB, 152-163, 1991.
- Chedin, A., N. Husson, N.A. Scott, I. Cohen-Hallaleh and A. Beroir, The GEISA data bank 1984 version, *Internal note LMD*, 127, Palaiseau (France), 1986.
- Chylek, P., and J. Wong, Effect of absorbing aerosols on global radiation budget, *Geophys. Res. Lett.*, 22, 929-931, 1995.

References

- Clough, S.A., F.X. Kneizys, and R.W. Davies, Line shape and the water vapor continuum, *Atmos. res.*, 23, 229-241, 1989.
- Crutzen, P.J., and P.H. Zimmermann, The changing photochemistry of the troposphere, *Tellus*, 43AB, 136-151, 1991.
- Dentener, F.J., and P.J. Crutzen, Reaction of N₂O₅ on tropospheric aerosols: Impact on the global distributions of NO_x, O₃ and OH, *J. Geophys. Res.*, 98, 7149-7163, 1993.
- Dentener, F.J., and P.J. Crutzen, A three-dimensional model of the global ammonia cycle, *J. Atmos. Chem.*, 19, 331-369, 1994.
- Dentener, F.J., R. Hein, and G.-J. Roelofs, A comparison of background ozone concentrations calculated by the three dimensional models ECHAM, MOGUNTIA and TM2 with measurements, *Rep. CM-88*, Dep. of Meteorol., Stockholm Univ., Stockholm, 1995.
- Dentener, F.J., G.R. Carmichael, Y. Zhang, J. Lelieveld, and P.J. Crutzen, The role of mineral aerosol as a reactive surface in the global troposphere, *J. Geophys. Res.*, 101, 22869-22889, 1996.
- Dickinson, R., Solar variability in the lower atmosphere *Bull. Am. Met. Soc.*, 56, 1240-1248, 1975.
- Dickinson, R.E. and R.J. Cicerone, Future global warming from atmospheric trace gases, *Nature*, 319, 109-115, 1986.
- Ellingson, R.G., and Y. Fouquart, Radiation and Climate: The intercomparison of radiation codes in climate models (ICRCCM), *Rep. WCRP-39*, 38 pp, WMO, Geneva, 1990.
- Ellingson, R.G., J. Ellis, and S. Fels, The intercomparison of radiation codes used in climate models: longwave results, *J. Geophys. Res.*, 96, 8929-8953, 1991.
- Emsley, J., Cool reception for warming predictions, *New Scientist*, 19, October 1994.
- European Science and Environment Forum (ESEF), *The global warming debate*, edited by J. Emsley, 288 pp., Bourne Press Lim., Bournemouth, Dorset, UK, 1996.
- Fleming, J.R., Historical perspectives on climate change, 194 pp, Oxford Univ. Press, 1998.
- Fortuin, J.P.F., R. van Dorland, W.M.F. Wauben, and H. Kelder, Greenhouse effects of aircraft emissions as calculated by a radiative transfer model, *Ann. Geophys.*, 13., 413-418, 1995a.
- Fortuin, J.P.F., R. van Dorland, and H. Kelder, Concurrent ozone and temperature trends derived from ozonesonde stations, in *Atmospheric Ozone as a Climate Gas*, edited by W.-C. Wang and I.S.A. Isaksen, pp. 131-144, NATO ASI Ser., Vol I 32, Springer-Verlag, New York, 1995b.

References

- Fouquart, Y. and B. Bonnel, Computations of solar heating of the earth's atmosphere: a new parameterization, *Beitr.Phys.Atmosph.*, 53, 35-62, 1980.
- Friis-Christensen, E., and K. Lassen, Length of the solar cycle: an indicator of solar activity closely associated with climate, *Science*, 254, 698-700, 1991.
- Garratt, J.R., and A.J. Prata, Downwelling longwave fluxes at continental surfaces - a comparison of observations with GCM simulations and implications for the global land-surface radiation budget, *J. Climate*, 9, 646-655, 1996.
- Gilliland, R.L., Solar, volcanic, and CO₂ forcing of recent climatic changes, *Climatic change*, 4, 111-131, 1982.
- Giorgetta, M., and M. Wild, The water vapour continuum and its representation in ECHAM4, *Report 162*, MPI, Hamburg, Germany, 1995.
- Goody, R.M, and Y.L. Yung, Atmospheric radiation; Theoretical basis, 520 pp., Oxford Univ. Press, 1989.
- Haigh, J.D., The role of stratospheric ozone in modulating the solar radiative forcing of climate, *Nature*, 370, 544-546, 1994.
- Hansen, J.E., M. Sato, A. Lacis, and R. Ruedy, Climatic impact of ozone change, paper presented at workshop on The Impact on Climate of Ozone Change and Aerosols, Intergovernmental Panel on Climate Change working group I and Int. Ozone Assess. Panel, Hamburg, Germany, May 1993.
- Hauglustaine, D.A., C. Granier, G.P. Brasseur, and G. Megie, The importance of atmospheric chemistry in the calculation of radiative forcing on the climate system, *J. Geophys. Res.*, 99, 1173-1186, 1994.
- Hoffert, M., A.J. Callegari, and C-T. Hsieh, The role of deep-sea heat storage in the secular response to climate forcing, *J. Geophys. Res.*, 85, 6667-6679, 1980.
- Howard, J.N., D.L. Burch, and D. Williams, Near-infrared transmission through synthetic atmospheres, *Geophys. Res. Papers, No. 40, AFCRC-TR-55-213*, 244 pp., Air Force Cambridge Research Center, 1955.
- Hoyt, D.V., and K.H. Schatten, A discussion of plausible solar irradiance variations, 1700-1992, *J. Geophys. Res.*, 98, 18,895-18,906, 1993
- Husson, N., A. Chedin, N.A. Scott, The GEISA spectroscopic line parameters data bank in 1984, *Ann. Geophys.*, 4, A, 2, 185-190, 1986.
- Idso, S.B., The climatological significance of a doubling of earth's atmospheric carbon dioxide concentration, *Science*, 207, 1462-1463, 1980.

References

- Intergovernmental Panel on Climate Change (IPCC), *Climate Change: the IPCC Scientific assessment*, edited by J.T. Houghton, G.J. Jenkins and J.J. Ephraums, 365 pp., Cambridge Univ. Press, Cambridge, UK, 1990.
- Intergovernmental Panel on Climate Change, *Climate Change 1992: The Supplementary Report to the IPCC Scientific assessment*, J.T. Houghton, B.A. Callander and S.K. Varney (Eds.), 200 pp., WMO/UNEP, Cambridge University Press, Cambridge, UK, 1992.
- Intergovernmental Panel on Climate Change, *Climate Change 1994: Radiative Forcing of Climate Change and An Evaluation of the IPCC IS92 Emission Scenarios*, edited by J.T. Houghton, L.G. Meira Filho, J. Bruce, Hoesung Lee, B.A. Callander, E. Haites, N. Harris and K. Maskell (Eds.), 340 pp., Cambridge Univ. Press, Cambridge, UK, 1994.
- Intergovernmental Panel on Climate Change, *IPCC Second Scientific Assessment of Climate Change*, edited by J.T. Houghton, L.G. Meira Filho, B.A. Callander, N. Harris, A. Kattenberg and K. Maskell, 572 pp., Cambridge Univ. Press, Cambridge, UK, 1995.
- Intergovernmental Panel on Climate Change, *An introduction to simple climate models used in the IPCC second assessment report*, edited by J.T. Houghton, L.G. Meira Filho, D.J. Griggs, and K. Maskell, 52 pp., Cambridge Univ. Press, Cambridge, UK, 1997.
- Jones, P.D., Hemispheric surface air temperatures: a reanalysis and update to 1993, *J. Climate*, 7, 1794-1802, 1994.
- Kanakidou, M., and P.J. Crutzen, Scale problems in global tropospheric chemistry modeling: Comparison of results obtained with a three-dimensional model adopting longitudinally uniform and varying emissions of NO_x and NMHC, *Chemosphere*, 26, 787-801, 1993.
- Kelly, P.M., and T.M.L. Wigley, Solar cycle length, greenhouse forcing and global climate, *Nature*, 360, 328-330, 1992.
- Kiehl, J.T., and V. Ramanathan, Radiative heating due to increased CO₂: the role of H₂O continuum absorption in the 12-18 μm region, *J. Atm. Sci.*, 39, 2923-2926, 1982.
- Kiehl, J.T., and B.P. Briegleb, The relative roles of sulfate aerosols and greenhouse gases in climate forcing, *Science*, 260, 311-314, 1993.
- Koepke, P., M. Hess, I. Schult, and E.P. Shettle, Global aerosol data set, *Report*, 243, MPI, Hamburg, Germany, 1997.
- Kohsiek, W., and A.C.A.P. van Lammeren, Pyrgeometer formula, *Appl. Opt.*, 36, 5984-5986, 1997.
- Lacis, A.A., D.J. Wuebbles, and J.A. Logan, Radiative forcing of climate by changes in the vertical distribution of ozone, *J. Geophys. Res.*, 95, 9971-9981, 1990.

References

- Lacis, A.A., J.E. Hansen, and M. Sato, Climate forcing by stratospheric aerosols, *Geophys. Res. Lett.*, *19*, 1607-1610, 1992.
- Langner, J., and H. Rodhe, A global three-dimensional model of the tropospheric sulfur cycle, *J. Atmos. Chem.*, *13*, 225-263, 1991.
- Lean, J., Variations in the sun's radiative output, *Rev. of Geophys.*, *29*, 505-535, 1991.
- Lelieveld, J., P.J. Crutzen, and H. Rodhe, Zonal average cloud characteristics for global atmospheric chemistry modeling, *Rep. CM-76.*, 54 pp., Dep. of Meteorol., Univ. of Stockholm, Stockholm, 1989.
- Lelieveld, J., and R. van Dorland, Ozone chemistry changes in the troposphere and consequent radiative forcing of climate, in *Atmospheric Ozone as a Climate Gas*, edited by W.-C. Wang and I.S.A. Isaksen, pp. 227-258, NATO ASI Ser., Vol I 32, Springer-Verlag, New York, 1995.
- Lenoble, J., Atmospheric radiative transfer, A. Deepak Publ., 532 pp., 1993.
- Liou, K.N., An introduction to atmospheric radiation, *Internat. Geophys. Ser.*, *26*, Acad. Press, N.Y., 392 pp., 1980.
- Luther, F.M., R.G. Ellingson, Y. Fouquart, S. Fels, N.A. Scott and W.J. Wiscombe, Intercomparison of radiation codes in climate models (ICRCCM), Longwave clear-sky results - a workshop summary, *Bull. Amer. Meteor. Soc.* *69*, 40-48 1988.
- Ma, Q., and R.H. Tipping, A far wing line shape theory and its application to foreign-broadened water continuum absorption (III), *J. Chem. Phys.*, *97*, 818-828, 1992.
- MacCracken, M.C. and F.M. Luther (Eds.), Projecting the climatic effects of increasing carbon dioxide, *Rep. DOE/ER-0237*, U.S. Dep. of Energy, Washington, D.C., 1985.
- Manabe, S., and R.F. Strickler, Thermal equilibrium of the atmosphere with a convective adjustment, *J. Atm. Sci.*, *21*, 361-385, 1964.
- Manabe, S., and R.T. Wetherald, Thermal equilibrium of the atmosphere with a given distribution of relative humidity, *J. Atm. Sci.*, *24*, 241-259, 1967.
- Manabe, S., and R.T. Wetherald, The effects of doubling the CO₂ concentration on the climate of a general circulation model, *J. Atm. Sci.*, *32*, 3-15, 1975.
- Marenco, A., H. Gouget, P. Nedelec, J.-P. Pages, and F. Karcher, Evidence of longterm increase in tropospheric ozone from Pic du Midi data series - consequences: Positive radiative forcing, *J. Geophys. Res.*, *99*, 16617-16632, 1994.
- Matthews, E., Vegetation, land-use and seasonal albedo data sets: Documentation and archived data tape, *NASA Tech. Memo.*, *86107*, 1984.

References

- McClatchey, R.A., R.W. Fenn, J.E.A. Selby, F.E. Voltz and J.S. Garing, Optical properties of the atmosphere, *AFCRL-TR-72-0497, Environmental Research Paper 411*, Bedford, Mass., 3rd ed., 108 pp., 1972.
- Mitchell, J.F.B., The 'greenhouse' effect and climate change, *Rev. Geophys.*, *27*, 115-139, 1989.
- Mitchell, J.F.B., R.A. Davis, W.J. Ingram, and C.A. Senior, On surface temperature, greenhouse gases and aerosols: Models and observations, *J. Clim.*, *8*, 2364-2386, 1995.
- Morcrette, J.-J., Sur la parameterisation du rayonnement dans les modeles de la circulation generale atmospherique. These de Doctorat d'Etat, Universite des Sciences et Techniques de Lille, pp. 630, 1984.
- Morcrette, J.-J. and Y. Fouquart, On the systematic errors in parameterized calculations of long-wave radiation transfer, *Quart. J. Roy. Meteor. Soc.*, *111*, 691-708, 1985.
- Morcrette, J.-J., L.D. Smith, and Y. Fouquart, Pressure and temperature dependence of the absorption in longwave radiation parameterizations, *Beitr. Phys. Atmosph.*, *59*, 455-469, 1986.
- Morcrette, J.-J., Description of the radiation scheme in the ECMWF model, *ECMWF Technical Memorandum 165*, 1989.
- Morcrette, J.-J., Radiation and cloud radiative properties in the European Centre for Medium-Range Weather Forecasting system, *J. Geophys. Res.*, *96*, 9121-9132, 1991.
- Nemesure, S., R. Wagener, and S.E. Schwartz, Direct shortwave forcing of climate by the anthropogenic sulfate aerosol: Sensitivity to particle size, composition and relative humidity, *J. Geophys. Res.*, *100*, 26105-26116, 1995.
- Nordstrom, R.J., and M.E. Thomas, The water vapor continuum as wings of strong absorption lines, in *Atmospheric Water Vapor*, A. Deepak, T.D. Wilkerson, and L.H. Ruhnke (Eds.), Acad. Press., London, 77-100, 1980.
- Oort, A.H., Global atmospheric circulation statistics, protect 1958-1973, *NOAA Prof. Pap. 14*, U.S. Gov. Print. Off., Washington D.C., 1983
- Oort, A.H., and H. Liu, Upper air temperature trends over the globe, 1958-1989, *J. Climate*, *6*, 292-307, 1993.
- Paltridge, G.W., and C.M.R. Platt, Radiative processes in meteorology and climatology, Elsevier Scient. Publ., N.Y., 318 pp., 1976.
- Peixoto, J.P. and A.H. Oort, Physics of climate, AIP, New York, 520 pp., 1992.
- Philipona, R., C. Fröhlich, and C. Betz, Characterization of pyrgeometers and the accuracy of atmospheric longwave radiation measurements, *Appl. Opt.*, *34*, 1598-1605, 1995.

References

- Philipona, R., C. Fröhlich, K. Dehne, J. DeLuisi, J. Augustine, E. Dutton, D. Nelson, B. Forgan, P. Novotny, J. Hickey, S.P. Love, S. Bender, B. McArthur, A. Ohmura, J.H. Seymour, J.S. Foot, M. Shiobara, F.P.J. Valero and A.W. Strawa, The Baseline Surface Radiation Network pyrgeometer round-robin calibration experiment, *J. Atmos. Ocean. Technol.*, *15*, 687-696, 1998.
- Pilewskie, P. and F.P.J. Valero, Direct observations of excess solar absorption by clouds, *Science*, *267*, 1626-1629, 1995.
- Pilinis, C., S.N. Pandis, and J.H. Seinfeld, Sensitivity of direct climate forcing by atmospheric aerosols to aerosol size and composition, *J. Geophys. Res.*, *100*, 18739-18754, 1995.
- Pinnock, S., and K.P. Shine, The effects of changes in HITRAN and uncertainties in the spectroscopy on infrared irradiance calculations, *J. Atm. Sc.*, *55*, 1950-1964, 1998.
- Plass, G.N., The carbon dioxide theory of climate change, *Tellus*, *8*, 140-154, 1956.
- Ramanathan, V., The role of earth radiation budget studies in climate and general circulation research, *J. Geophys. Res.*, *92*, 4075-4095, 1987.
- Ramanathan, V., L. Callis, R. Cess, J. Hansen, I. Isaksen, W. Kuhn, A. Lacis, F. Luther, J. Mahlman, R. Reck and M. Schlesinger, Climate Chemical interactions and effects of changing atmospheric trace gases, *Rev. Geophys.*, *25*, 1441-1482, 1987.
- Ramanathan, V., R.D. Cess, E.F. Harrison, P. Minnis, B.R. Barkstrom, E. Ahmad, and D. Hartmann, Cloud-radiative forcing and climate: results from the Earth Radiation Budget Experiment, *Science*, *243*, 57-63, 1989.
- Ramaswamy, V., K.P. Shine, C. Leovy, W.-C. Wang, H. Rodhe, and D. Wuebbles, Radiative forcing of climate, *WMO Rep.*, *25*, Scientific assessment of ozone depletion, 1991.
- Ramaswamy, V., and C-T. Chen, Climate forcing-response relationships for greenhouse and shortwave radiative perturbations, *Geophys. Res. Lett.*, *24*, 667-670, 1997.
- Randall, D.A., R.D. Cess, J.P. Blanchet, G.J. Boer, D.A. Dazlich, A.D. Del Genio, M. Deque, V. Dimnikov, V. Galin, S.J. Ghan, A.A. Lacis, H. Le Treut, Z.-X. Li, X.-Z. Liang, B.J. McAvaney, V.P. Meleshko, J.F.B. Mitchell, J.-J. Morcrette, G.L. Potter, L. Rikus, E. Roekner, J.F. Royer, U. Schlese, D.A. Sheinin, J. Slingo, A.P. Solokov, K.E. Taylor, W.M. Washington, R.T. Wetherald, I. Yagai, and M.-H. Zhang, Intercomparison and interpretation of surface energy fluxes in atmospheric general circulation models, *J. Geophys. Res.*, *97*, 3711-3724, 1992.
- Raval, A., and V. Ramanathan, Observational determination of the greenhouse effect, *Nature*, *342*, 758-761, 1989.

References

- Reid, G.C., Solar total irradiance variations and the global sea surface temperature record, *J. Geophys. Res.*, *96*, 2835-2844, 1991.
- Revelle, R., and H.E. Suess, Carbon dioxide exchange between atmosphere and ocean and the question of an increase of atmospheric CO₂ during the past decades, *Tellus*, *9*, 18-27, 1957.
- Ritter, B, Radiation in numerical weather prediction, Meteorological training course, *ECMWF Lecture note no. 3.2*, 84 pp., 1986.
- Roberts, R.E., J.E.A. Selby, and L.B. Biberman, Infrared continuum absorption by atmospheric water vapor in the 8-12 μm window, *Appl. Opt.*, *15*, 2085-2090, 1976.
- Rodgers, C.D. and C.D. Walshaw, The computation of infrared cooling rate in planetary atmospheres, *Quart. J. Roy. Meteor. Soc.*, *92*, 67-92, 1966.
- Rodgers, C.D., Some extensions and applications of the new random band model for molecular band transmission, *Quart. J. Roy. Meteor. Soc.*, *94*, 99-102, 1968.
- Rodhe, H., and R. Charlson, The legacy of Svante Arrhenius understanding the greenhouse effect, 276 pp., Royal Swedish Academy of Sciences, Stockholm Univ., 1998.
- Roeckner, E., K. Arpe, L. Bengtsson, M. Christoph, M. Claussen, L. Dümenil, M. Esch, M. Giorgetta, U. Schlese, and U. Schulweida, The atmospheric general circulation model ECHAM-4: model description and simulation of present-day climate, *Rep. 218*, Max-Planck-Inst. for Meteorol., Hamburg, Germany, 1996.
- Roelofs, G.J., J. Lelieveld, and R. van Dorland, A three-dimensional chemistry/general circulation model simulation of anthropogenically derived ozone in the troposphere and its radiative climate forcing, *J. Geophys. Res.*, *102*, 23389-23401, 1997.
- Rossow, W.B., and Y.-C. Zhang, Calculation of surface and top of atmosphere radiative fluxes from physical quantities based on ISCCP data sets: 2. Validation and first results, *J. Geophys. Res.*, *100*, 1167-1197, 1995.
- Rothman, L.S., AFGL atmospheric absorption line parameters compilation: 1980 version, *Appl. Opt.*, *20*, 791-795, 1981.
- Rothman, L.S., C.P. Rinsland, A. Goldman, S.T. Massie, D.P. Edwards, J.-M. Flaud, A. Perrin, C. Camy-Peyret, V. Dana, J.-Y. Mandin, J. Schroeder, A. McCann, R.R. Gamache, R.B. Wattson, K. Yoshino, K.V. Chance, K.W. Jucks, I.R. Brown, V. Nemtchinov, and P. Varanassi, The HITRAN molecular spectroscopic database and HAWKS (HITRAN Atmospheric Workstation): 1996 edition, *J. Quant. Spectr. Rad. Transfer.*, 1998.

References

- Santer, B.D., K.E. Taylor, T.M.L. Wigley, P.D. Jones, D.J. Karoly, J.F.B. Mitchell, J.E. Penner, V. Ramaswamy, M.D. Schwartzkopf, R.J. Stouffer and S. Tett, A search for human influences on the thermal structure of the atmosphere, *Nature*, 382, 39-46, 1996.
- Sato, M., J.E. Hansen, M.P. McCormick, and J.B. Pollack, Stratospheric aerosol optical depths, 1850-1990, *J. Geophys. Res.*, 98, 22987-22994, 1993.
- Schuermans, C.J.E., Atmospheric trace gases and climate change, in proceedings of *International Congress on Nature Management and Sustainable Development*, Groningen, The Netherlands, 6-9 December, 1988.
- Shine, K.P., B.P. Briegleb, A.S. Grossman, D. Hauglustaine, H. Mao, V. Ramaswamy, M.D. Schwarzkopf, R. van Dorland, and W.-C. Wang, Radiative forcing due to changes in ozone: a comparison of different codes, in *Atmospheric Ozone as a Climate Gas*, edited by W.-C. Wang and I.S.A. Isaksen, pp. 373-396, NATO ASI Ser., Vol I 32, Springer-Verlag, New York, 1995.
- Smith, M.H., B. Fridovich and K.N. Rao, Intensities and collision broadening parameters from infrared spectra, *Molecular spectroscopy, Modern Research*, 3, chapter 3, Academic Press, New York, 1985.
- Soon, W.H., E.S. Posmentier, and S.L. Baliunas, Inference of solar irradiance variability from terrestrial temperature changes, 1880-1993: An astronomical application of the sun-climate connection, *Astr. Journal*, 472, 891-902, 1996.
- Stephens, G.L., The parameterization of radiation for numerical weather prediction and climate models, *Monthly Weather Rev.*, 112, 826-867, 1984.
- Svensmark, H., and E. Friis-Christensen, Variation of cosmic ray flux and global cloud coverage -a missing link in solar-climate relationships, *J. Atm. and Solar-Terr. Phys.*, 59, 1125-1232, 1997.
- Tanré, D., J.F. Geleyn, and J. Slingo, First results of the introduction of an advanced aerosol-radiation interaction in the ECMWF low resolution global model, in *Aerosols and their climatic effects*, H.E. Gerber, and A. Deepak (Eds.), 133-177, 1984.
- Taylor, K.E., and J.E. Penner, Response of the climate system to atmospheric aerosols and greenhouse gases, *Nature*, 369, 734-737, 1994.
- Ten Brink, H.M., J.P. Veefkind, A. Waijers-IJpenlaan, and J.C. van der Hage, Aerosol light-scattering in the Netherlands, *Atmos. Environ.*, 30, 4251-4261, 1996.
- Van Dorland, R. and J.P.F. Fortuin, Simulation of the observed stratospheric temperature trends 1967-1987 over Antarctica due to ozone hole deepening, in *Non CO₂ Greenhouse Gases*, edited by J. van Ham et al., pp. 237-245, Kluwer Acad., Norwell, Mass., 1994.

References

- Van Dorland, R., Is carbon dioxide absorption saturated?, Debate on the radiative effects of increasing concentrations of carbon dioxide, Dutch Engineers Association, The Hague, The Netherlands, 26 September 1995, *KNMI Personal Memorandum, AO-95-04*, 1995.
- Van Dorland, R., F.J. Dentener, and J. Lelieveld, Radiative forcing due to tropospheric ozone and sulfate aerosols, *J. Geophys. Res.*, *102*, 28079-28100, 1997.
- Van Dorland, R., Het broeikaseffect ter discussie; De rol van CO₂ in de broeikasverwarming, *Zenit*, *24*, 30-35, 1997.
- Van Dorland, R., Is de aarde warmer geworden?, *Zenit*, *25*, 534-535, 1998.
- Van Lammeren, A.C.A.P., A. Feijt, J. Konings, E. van Meijgaard, and A.P. van Ulden, Combination of ground based and satellite cloud observations on a routine basis, *submitted to Contr. Atm. Phys.*, 1998.
- Warren, S.G., C.J. Hahn, and J. London, Simultaneous occurrence of different cloud types, *J. Appl. Meteorol.*, *24*, 658-667, 1985.
- Wigley, T.M.L., and S.C.B. Raper, Implications for climate and sealevel of revised IPCC emission scenarios, *Nature*, *357*, 293-300, 1992.
- Wild, M., A. Ohmura, H. Gilgen, and E. Roeckner, Validation of general circulation model simulated radiative fluxes using surface observations, *J. Climate*, *8*, 1309-1324, 1995.
- World Meteorological Organization (WMO), Scientific assessment of ozone depletion, *Global Ozone Res. and Monit. proj. Rep. 25*, Geneva, 1992.
- Yamamoto, G., On a radiation chart, *Sci. Rep. of the Tohoku Univ., Ser. 5*, *4*, 9-23, 1952.
- Zhang, M.-H., R.D. Cess, and X. Jing, Concerning the interpretation of enhanced shortwave absorption using monthly-mean Earth Radiation Budget Experiment/Global Energy Balance Archive measurements, *J. Geophys. Res.*, *102*, 25899-25905, 1997.
- Zhang, Q., W.H. Soon, S.L. Baliunas, G.W. Lockwood, B.A. Skiff, and R.R. Radick, A method of determining possible brightness variations of the Sun in past centuries from observations of solar-type stars, *Astrophys. J.*, *427*, L111-L114, 1994.
- Zimmermann, P.H., MOGUNTIA, a handy global tracer model, in *Air Pollution Modelling and Its Applications, Proceedings NATO/CCMS Meeting in Lindau, FRG, 6-10 April 1987*, pp. 503-608, D. Reidel, Norwell, Mass., 1987.

List of Acronyms and Abbreviations

AFEAS	Alternative Fluorocarbons Environmental Acceptibility Study
AFGL	Air Force Geophysical Laboratory
ECBILT	Atmosphere Ocean Sea-ice Climate Model developed at KNMI
ECHAM	European Centre/Hamburg climate model
ECMWF	European Centre for Medium-Range Weather Forecasts
ERBE	Earth Radiation Budget Experiment
ESEF	European Science and Environment Forum
FDH	Fixed Dynamical Heating
GADS	Global Aerosol Data Set
GCM	General Circulation Model
GEISA	Gestion et Étude des Informations Spectroscopiques Atmosphériques
HITRAN	High Resolution Transmission Molecular Absorption Database
IMAU	Institute for Marine and Atmospheric research Utrecht
ICRCCM	InterComparison of Radiation Codes for Climate Models
IPCC	Intergovernmental Panel on Climate Change
IS92a	IPCC Scenario for trace gas emissions
KNMI	Royal Netherlands Meteorological Institute
KRCM	KNMI Radiative-Convective Model
LBL	Line By Line radiative transfer model
LW	Longwave
MLS	Mid-Latitude Summer atmospheric profile
MOGUNTIA	Model Of the General UNiversal Tracer transport In the Atmosphere
MPI	Max Planck Institute
NBM	Narrow Band radiative transfer Model
NIR	Near Infrared spectral range
NOAA	National Oceanic and Atmospheric Administration (USA)
RCM	Radiative-Convective Model
RH	Relative Humidity
RTE	Radiative Transfer Equation
SINDICATE	Study of INdirect and DIRECT Climate influences of Anthropogenic Trace Gas Emissions
SAW	Sub-Arctic Winter atmospheric profile
SCL	Solar Cycle Length
SIDC	Sunspot Index Data Centre
SFC	Surface
SLA	Strong Line Approximation

List of Acronyms and Abbreviations

SW	Shortwave
TEBEX	Tropospheric Energy Budget EXperiment
TOA	Top of the Atmosphere
TRP	Tropopause
UV	Ultraviolet spectral range
VIS	Visual spectral range
WASO	Water Soluble aerosol
WBM	Wide Band radiative transfer Model
WLA	Weak Line Approximation
WMO	World Meteorological Organization

List of Publications

- Feijt, A.J., R. van Dorland, A.C.A.P. van Lammeren, E. van Meijgaard, and P. Stammes, Cloud-Radiation-Hydrological interactions: Measuring and Modelling, *KNMI Scientific Report, WR 94-04*, 1994.
- Fortuin, J.P.F., R. van Dorland, W.M.F. Wauben, and H. Kelder, Greenhouse effects of aircraft emissions as calculated by a radiative transfer model, *Ann. Geophys.*, *13*, 413-418, 1995.
- Fortuin, J.P.F., R. van Dorland, and H. Kelder, Concurrent ozone and temperature trends derived from ozonesonde stations, in *Atmospheric Ozone as a Climate Gas*, edited by W.-C. Wang and I.S.A. Isaksen, pp. 131-143, NATO ASI Ser., Vol I 32, Springer-Verlag, New York, 1995.
- Fortuin, J.P.F., W.M.F. Wauben, R. van Dorland, and H. Kelder, Greenhouse effects of aircraft emissions, *Proceedings of 7th Global Warming Int. Conference*, Vienna, 1996.
- Kelder, H., M. Allaart, R. van Dorland, J.P.F. Fortuin, L.C. Heijboer, A. Jeuken, P. van Velthoven, and G. Verver, KNMI contributions to global modelling of transport, atmospheric composition and radiation, in *Tropospheric modelling and emission estimation*, edited by A. Ebel, R. Friedrich, and H. Rodhe, Springer, Heidelberg, 1997.
- Lelieveld, J., and R. van Dorland, Ozone chemistry changes in the troposphere and consequent radiative forcing of climate, in *Atmospheric Ozone as a Climate Gas*, edited by W.-C. Wang and I.S.A. Isaksen, pp. 227-258, NATO ASI Ser., Vol I 32, Springer-Verlag, New York, 1995.
- Roelofs, G.J., J. Lelieveld, and R. van Dorland, A three-dimensional chemistry/general circulation model simulation of anthropogenically derived ozone in the troposphere and its radiative climate forcing, *J. Geophys. Res.*, *102*, 23,389-23,401, 1997.
- Schaeffer, M., F. Selten, and R. van Dorland, Linking IMAGE and ECBILT, *RIVM report, 4815008008*, 1998.
- Shine, K.P., B.P. Briegleb, A.S. Grossman, D. Hauglustaine, H. Mao, V. Ramaswamy, M.D. Schwarzkopf, R. van Dorland, and W.-C. Wang, Radiative forcing due to changes in ozone: a comparison of different codes, in *Atmospheric Ozone as a Climate Gas*, edited by W.-C. Wang and I.S.A. Isaksen, pp. 373-396, NATO ASI Ser., Vol I 32, Springer-Verlag, New York, 1995.
- Van Dorland, R. and J.-J. Morcrette, A comparison of two spectroscopic compilations using longwave radiation models, *KNMI Personal Memorandum, FM-93-04*, 1993.

List of Publications

- Van Dorland, R. and J.P.F. Fortuin, Simulation of the observed stratospheric temperature trends 1967-1987 over Antarctica due to ozone hole deepening, in *Non CO₂ Greenhouse Gases*, edited by J. van Ham et al., pp. 237-245, Kluwer Academic Publishers, 1994.
- Van Dorland, R., Klimaatvoorspellingen, in *Heeft de aarde koorts?*, edited by L. Bruning, A. Jansen, J. Luyten, and P. van Vlaardingen, Stichting Universum, Utrecht, 1994.
- Van Dorland, R., Is carbon dioxide absorption saturated?, Debate on the radiative effects of increasing concentrations of carbon dioxide, Dutch Engineers Association, The Hague, The Netherlands, 26 September 1995, *KNMI Personal Memorandum, AO-95-04*, 1995.
- Van Dorland, R., F.J. Dentener, and J. Lelieveld, Radiative forcing due to tropospheric ozone and sulfate aerosols, *J. Geophys. Res.*, 102, 28,079-28,100, 1997.
- Van Dorland, R., Het broeikaseffect ter discussie; De rol van CO₂ in de broeikasverwarming, *Zenit*, 24, 30-35, 1997.
- Van Dorland, R., and A.P. van Ulden, Natural and anthropogenic variations in the radiation balance, *Symposium proceedings Sun and Climate: the influence of variations in solar activity on climate*, 1998.
- Van Dorland, R., Klimaat en zonneschijn, *Zenit*, 25, 156-161, 1998.
- Van Dorland, R., Geen vuiltje aan de lucht: Klimaat effecten van vliegverkeer, *Zenit*, 25, 330-333, 1998.
- Van Dorland, R., Is de aarde warmer geworden?, *Zenit*, 25, 534-535, 1998.
- Van Ulden, A.P., and R. van Dorland, Statistical relations between solar activity, anthropogenic greenhouse effect and global temperatures from 1856 to 1997, *Symposium proceedings, Sun and Climate: the influence of variations in solar activity on climate*, 1998.
- Van Velthoven, P.F.J., J.P.F. Fortuin, R. van Dorland, and H. Kelder, Simulation of stratospheric cooling above Antarctica, *Proceedings Strateole workshop, 9-10 Oct*, 1995.

Curriculum Vitae

Rob van Dorland (geboren op 17 januari 1959 te Utrecht) volgde zijn middelbare school opleiding aan het Stedelijk Gymnasium in Utrecht. In 1978 werd het Gymnasium β diploma behaald. In deze periode was hij actief lid van de Jongeren WerkGroep (JWG) van de Nederlandse Vereniging voor Weer- en Sterrenkunde. Ofschoon de interesse in het begin voornamelijk bij de sterrenkunde lag, groeide gaandeweg de belangstelling voor de meteorologie. Dit uitte zich onder andere in het geven van cursussen weerkunde tijdens de JWG zomerkampen.

Hierna volgde hij de kandidaatsopleiding Natuurkunde met met bijvak Geofysica aan de Rijksuniversiteit Utrecht, gevolgd door de doctoraalstudie Meteorologie en Fysische Oceanografie met bijvakken Signaalverwerking en Milieukunde. De titel van het afstudeeronderzoek luidde: *Topografisch geforceerde stationaire planetaire golven met een barokken karakter*. Het doctoralexamen Meteorologie werd op 25 januari 1988 afgelegd. Gedurende de laatste vier jaar van deze studie is hij bij het IMAU werkzaam geweest als studentassistent voor het tweedejaars practicum Meteorologie, waarvoor tevens een syllabus geschreven is. Later is dit uitgebreid met het practicum Oceanografie.

Sinds 1988 is hij verbonden aan het KNMI als wetenschappelijk onderzoeker. Onderwerp van onderzoek is de stralingshuishouding van het aarde-atmosfeersysteem en in het bijzonder de analyse van het (versterkte) broeikas effect. Hij is betrokken (geweest) bij de NOP projecten *Clouds-Radiation-Hydrologic cycle interactions in a limited-area model*, *Aerosol: cycle and influence on the radiation balance*, *Assessment van de 'Deense theorie' over de invloed van de zon op het klimaat*, alsook het recent toegekende project *Research on a mechanism by which enhanced UV-radiation of the active sun effects weather and climate* en bij het SRON project *Aerosol retrieval from multi-spectral measurements from satellites*. Tevens heeft hij deelgenomen aan het Europese project SINDICATE (*Study of INdirect and DIrect Climate influences of Anthropogenic Trace gas Emissions*).

Sinds enkele jaren is hij betrokken bij de organisatie van de cursus weerkunde van de Volkssterrenwacht Utrecht. Voorts maakt hij deel uit van de redactie van het populair wetenschappelijke (maand)blad Zenit met als taak het redigeren en schrijven van artikelen over de Meteorologie.

Hoewel het van meet af aan de bedoeling was om te promoveren op een onderwerp, dat gerelateerd is aan zowel atmosferisch stralingstransport als de menselijke beïnvloeding van het klimaat, zijn in begin 1995 de eerste concrete stappen ondernomen. Uiteindelijk heeft dit geleid tot de totstand koming van het voorliggende proefschrift, getiteld *Radiation and Climate: from radiative transfer modelling to global temperature response*.

